

Machine learning approximation algorithms for high-dimensional fully nonlinear partial differential equations and second-order backward stochastic differential equations

Christian Beck¹, Weinan E², and Arnulf Jentzen³

¹ETH Zurich (Switzerland), e-mail: christian.beck (at) math.ethz.ch

²Beijing Institute of Big Data Research (China), Princeton University (USA),
and Peking University (China), e-mail: weinan (at) math.princeton.edu

³ETH Zurich (Switzerland), e-mail: arnulf.jentzen (at) sam.math.ethz.ch

September 19, 2017

Abstract

High-dimensional partial differential equations (PDE) appear in a number of models from the financial industry, such as in derivative pricing models, credit valuation adjustment (CVA) models, or portfolio optimization models. The PDEs in such applications are high-dimensional as the dimension corresponds to the number of financial assets in a portfolio. Moreover, such PDEs are often fully nonlinear due to the need to incorporate certain nonlinear phenomena in the model such as default risks, transaction costs, volatility uncertainty (Knightian uncertainty), or trading constraints in the model. Such high-dimensional fully nonlinear PDEs are exceedingly difficult to solve as the computational effort for standard approximation methods grows exponentially with the dimension. In this work we propose a new method for solving high-dimensional fully nonlinear second-order PDEs. Our method can in particular be used to sample from high-dimensional nonlinear expectations. The method is based on (i) a connection between fully nonlinear second-order PDEs and second-order backward stochastic differential equations (2BSDEs), (ii) a merged formulation of the PDE and the 2BSDE problem, (iii) a temporal forward discretization of the 2BSDE and a spatial approximation via deep neural nets, and (iv) a stochastic gradient descent-type optimization procedure. Numerical results obtained using TENSORFLOW in PYTHON illustrate the efficiency and the accuracy of the method in the cases of a 100-dimensional Black-Scholes-Barenblatt equation,

a 100-dimensional Hamilton-Jacobi-Bellman equation, and a nonlinear expectation of a 100-dimensional G -Brownian motion.

Keywords: deep learning, second-order backward stochastic differential equation, 2BSDE, numerical method, Black-Scholes-Barentblatt equation, Knightian uncertainty, Hamiltonian-Jacobi-Bellman equation, HJB equation, nonlinear expectation, G -Brownian motion

Contents

1	Introduction	3
2	Main ideas of the deep 2BSDE method	5
2.1	Fully nonlinear second-order PDEs	6
2.2	Connection between fully nonlinear second-order PDEs and 2BSDEs	6
2.3	Merged formulation of the PDE and the 2BSDE	7
2.4	Forward-discretization of the merged PDE-2BSDE system	7
2.5	Deep learning approximations	8
2.6	Stochastic gradient descent-type optimization	9
2.7	Framework for the algorithm in a specific case	10
3	The deep 2BSDE method in the general case	11
3.1	Fully nonlinear second-order PDEs	12
3.2	Connection between fully nonlinear second-order PDEs and 2BSDEs	12
3.3	Merged formulation of the PDE and the 2BSDE	14
3.4	Forward-discretization of the merged PDE-2BSDE system	15
3.5	Deep learning approximations	16
3.6	Stochastic gradient descent-type optimization	17
3.7	Framework for the algorithm in the general case	17
4	Examples	20
4.1	Allen-Cahn equation with plain gradient descent and no batch normalization	20
4.2	Setting for the deep 2BSDE method with batch normalization and Adam .	22
4.3	A 100-dimensional Black-Scholes-Barenblatt equation	23
4.4	A 100-dimensional Hamilton-Jacobi-Bellman equation	26
4.5	A 50-dimensional Allen-Cahn equation	27
4.6	G -Brownian motions in 1 and 100 space-dimensions	30

A	Source codes	34
A.1	A PYTHON code for the deep 2BSDE method used in Subsection 4.1 . . .	34
A.2	A MATLAB code for the Branching diffusion method used in Subsection 4.1	38
A.3	A PYTHON code for the deep 2BSDE method used in Subsection 4.3 . . .	40
A.4	A MATLAB code for the classical Monte Carlo method used in Subsection 4.4	46
A.5	A MATLAB code for the finite differences method used in Subsection 4.6 .	46

1 Introduction

Partial differential equations (PDE) play an important role in an abundance of models from finance to physics. Objects as the wave function associated to a quantum physical system, the value function describing the fair price of a financial derivative in a pricing model, or the value function describing the expected maximal utility in a portfolio optimization problem are often given as solutions to nonlinear PDEs. Roughly speaking, the nonlinearities in the above mentioned PDEs from financial engineering applications appear due to certain nonlinear effects in the trading portfolio (the trading portfolio for hedging the financial derivative claim in the case of derivative pricing problems and the trading portfolio whose utility has to be maximized in the case of portfolio optimization problems); see, e.g., [7, 9, 37, 45, 66, 71] for derivative pricing models with different interest rates for borrowing and lending, see, e.g., [24, 53] for derivative pricing models incorporating the default risk of the issuer of the financial derivative, see, e.g., [4, 5, 109] for models for the pricing of financial derivatives on untradable underlyings such as financial derivatives on the temperature or mortality-dependent financial derivatives, see, e.g., [1, 36, 83] for models incorporating that the trading strategy influences the price processes through demand and supply (so-called large investor effects), see, e.g., [39, 50, 70, 94] for models taking transaction costs in the trading portfolio into account, and see, e.g., [2, 50] for models incorporating uncertainties in the model parameters for the underlyings (Knightian uncertainty). The PDEs emerging from such models are often high-dimensional as the associated trading portfolios frequently contain a whole basket of financial assets (see, e.g., [7, 24, 39]). These high-dimensional nonlinear PDEs are typically exceedingly difficult to solve approximatively. Nonetheless, there is a strong demand from the financial engineering industry to approximatively compute the solutions of such high-dimensional nonlinear parabolic PDEs due to the above mentioned practical relevance of these PDEs.

There are a number of numerical methods for solving nonlinear parabolic PDEs approximatively in the literature. Some of these methods are deterministic approximation methods and others are random approximation methods which rely on suitable probabilistic representations of the corresponding PDE solutions such as probabilistic representations based on backward stochastic differential equations (BSDEs) (cf., e.g., [10, 11, 42, 85, 86, 87, 88]), probabilistic representations based on second-order backward stochastic differential equations (2BSDEs) (cf., e.g., [22]), probabilistic representations based on branching diffusions

(cf., e.g., [53, 54, 55, 77, 102, 108]), and probabilistic representations based on extensions of the classical Feynman-Kac formula (cf., e.g., [34, 58, 84]). We refer, e.g., to [23, 30, 65, 69, 95, 103, 104, 106] for deterministic approximation methods for PDEs, to [3, 6, 7, 13, 18, 19, 20, 21, 25, 26, 27, 28, 31, 32, 43, 44, 45, 46, 47, 48, 56, 64, 71, 72, 73, 74, 75, 81, 82, 93, 98, 99, 100, 105, 111] for probabilistic approximation methods for PDEs based on temporal discretizations of BSDEs, to [33, 52] for probabilistic approximation methods for PDEs based on suitable deep learning approximations for BSDEs, to [40, 110] for probabilistic approximation methods for BSDEs based on sparse grid approximations, to [14, 41] for probabilistic approximation methods for BSDEs based on Wiener Chaos expansions, to [12, 22, 38, 49, 62, 112] for probabilistic approximation methods for PDEs based on temporal discretization of 2BSDEs, to [17, 53, 54, 55, 96, 107] for probabilistic approximation methods for PDEs based on branching diffusion representations, and to [34, 35] for probabilistic approximation methods based on extensions of the classical Feynman-Kac formula.

Most of the above named approximation methods are, however, only applicable in the case where the PDE/BSDE dimension d is rather small or work exclusively in the case of serious restrictions on the parameters or the type of the considered PDE (e.g., small nonlinearities, small terminal/initial conditions, semilinear structure of the PDE). The numerical solution of a high-dimensional nonlinear PDE thus remains an exceedingly difficult task and there is only a limited number of situations where practical algorithms for high-dimensional PDEs have been developed (cf., e.g., [29, 33, 34, 35, 52, 54, 55, 101]). In particular, to the best of our knowledge, at the moment there exists no practical algorithm for high-dimensional fully nonlinear parabolic PDEs in the scientific literature.

In this work we intend to overcome this difficulty, that is, we propose a new algorithm for solving fully-nonlinear PDEs and nonlinear second-order backward stochastic differential equations 2BSDEs. Our method in particular can be used to sample from Shige Peng's nonlinear expectation in high space-dimensions (cf., e.g., [89, 90, 91, 92]). The proposed algorithm exploits a connection between PDEs and 2BSDEs (cf., e.g., Cheridito et al. [22]) to obtain a merged formulation of the PDE and the 2BSDE, whose solution is then approximated by combining a time-discretization with a neural network based deep learning procedure (cf., e.g., [8, 15, 16, 23, 30, 33, 51, 52, 59, 63, 65, 68, 67, 69, 78, 79, 95, 97]). Roughly speaking, the merged formulation allows us to formulate the original PDE problem as a learning problem. The random loss function for the deep neural network in our algorithm is, loosely speaking, given by the error between the prescribed terminal condition of the 2BSDE and the neural network based forward time discretization of the 2BSDE. A related deep learning approximation algorithm for PDEs of semilinear type based on forward BSDEs has been recently proposed in [33, 52]. A key difference between [33, 52] and the present work is that here we rely on the connection between fully nonlinear PDEs and 2BSDEs given by Cheridito et al. [22] while [33, 52] rely on the nowadays almost classical connection between PDEs and BSDEs (cf., e.g., [86, 85, 87, 88]). This is the reason why

the method proposed in [33, 52] is only applicable to semilinear PDEs while the algorithm proposed here allows to treat fully nonlinear PDEs and nonlinear expectations.

The remainder of this article is organized as follows. In Section 2 we derive (see Subsections 2.1–2.6 below) and formulate (see Subsection 2.7 below) a special case of the algorithm proposed in this work. In Section 3 the proposed algorithm is derived (see Subsections 3.1–3.5 below) and formulated (see Subsection 3.7 below) in the general case. The core idea is most apparent in the simplified framework in Subsection 2.7 (see Framework 2.1 below). The general framework in Subsection 3.7, in turn, allows for employing more sophisticated machine learning techniques (see Framework 3.2 below). In Section 4 we present numerical results for the proposed algorithm in the case of several high-dimensional PDEs. In Subsection 4.1 the proposed algorithm in the simplified framework in Subsection 2.7 is employed to approximatively calculate the solution of a 20-dimensional Allen-Cahn equation. In Subsections 4.3, 4.4, 4.5, and 4.6 the proposed algorithm in the general framework in Subsection 3.7 is used to approximatively calculate the solution of a 100-dimensional Black-Scholes-Barenblatt equation, the solution of a 100-dimensional Hamilton-Jacobi-Bellman equation, the solution of a 50-dimensional Allen-Cahn equation, and nonlinear expectations of G -Brownian motions in 1 and 100 space-dimensions. PYTHON implementations of the algorithms are provided in Section A.

2 Main ideas of the deep 2BSDE method

In Subsections 2.1–2.6 below we explain the main idea behind the algorithm proposed in this work which we refer to as *deep 2BSDE method*. This is done at the expense of a rather sketchy derivation and description. More precise and more general definitions of the deep 2BSDE method may be found in Sections 2.7 and 3.7 below. In a nutshell, the main ingredients of the deep 2BSDE method are

- (i) a certain connection between PDEs and 2BSDEs,
- (ii) a merged formulation of the PDE and the 2BSDE problem,
- (iii) a temporal forward discretization of the 2BSDE and a spatial approximation via deep neural nets, and
- (iv) a stochastic gradient descent-type optimization procedure.

The derivation of the deep 2BSDE method is mainly based on ideas in E, Han, & Jentzen [33] and Cheridito et al. [22] (cf., e.g., [33, Section 2] and [22, Theorem 4.10]). Let us start now by describing the PDE problems which we want to solve with the deep 2BSDE method.

2.1 Fully nonlinear second-order PDEs

Let $d \in \mathbb{N} = \{1, 2, 3, \dots\}$, $T \in (0, \infty)$, $u = (u(t, x))_{t \in [0, T], x \in \mathbb{R}^d} \in C^{1,2}([0, T] \times \mathbb{R}^d, \mathbb{R})$, $f \in C([0, T] \times \mathbb{R}^d \times \mathbb{R} \times \mathbb{R}^d \times \mathbb{R}^{d \times d}, \mathbb{R})$, $g \in C(\mathbb{R}^d, \mathbb{R})$ satisfy for all $t \in [0, T]$, $x \in \mathbb{R}^d$ that $u(T, x) = g(x)$ and

$$\frac{\partial u}{\partial t}(t, x) = f(t, x, u(t, x), (\nabla_x u)(t, x), (\text{Hess}_x u)(t, x)). \quad (1)$$

The deep 2BSDE method allows us to approximatively compute the function $u(0, x)$, $x \in \mathbb{R}^d$. To fix ideas we restrict ourselves in this section to the approximative computation of the real number $u(0, \xi) \in \mathbb{R}$ for some $\xi \in \mathbb{R}^d$ and we refer to Subsection 3.7 below for the general algorithm. Moreover, the deep 2BSDE method can easily be extended to the case of systems of fully nonlinear second-order parabolic PDEs but in order to keep the notational complexity as low as possible we restrict ourself to the scalar case in this work (cf. (1) above). Note that the PDE (1) is formulated as a terminal value problem. We chose the terminal value problem formulation over the in the PDE literature more common initial value problem formulation because, on the one hand, the terminal value problem formulation seems to be more natural in connection with second-order BSDEs (which we are going to use below in the derivation of the proposed approximation algorithm) and because, on the other hand, the terminal value problem formulation shows up naturally in financial engineering applications like the Black-Scholes-Barenblatt equation in derivative pricing (cf. Section 4.3). Clearly, terminal value problems can be transformed into initial value problems and vice versa; see, e.g., Remark 3.3 below.

2.2 Connection between fully nonlinear second-order PDEs and 2BSDEs

Let $(\Omega, \mathcal{F}, \mathbb{P})$ be a probability space, let $W : [0, T] \times \Omega \rightarrow \mathbb{R}^d$ be a standard Brownian motion on $(\Omega, \mathcal{F}, \mathbb{P})$ with continuous sample paths, let $\mathbb{F} = (\mathbb{F}_t)_{t \in [0, T]}$ be the normal filtration on $(\Omega, \mathcal{F}, \mathbb{P})$ generated by W , and let $Y : [0, T] \times \Omega \rightarrow \mathbb{R}$, $Z : [0, T] \times \Omega \rightarrow \mathbb{R}^d$, $\Gamma : [0, T] \times \Omega \rightarrow \mathbb{R}^{d \times d}$, and $A : [0, T] \times \Omega \rightarrow \mathbb{R}^d$ be \mathbb{F} -adapted stochastic processes with continuous sample paths which satisfy that for all $t \in [0, T]$ it holds \mathbb{P} -a.s. that

$$Y_t = g(\xi + W_T) - \int_t^T (f(s, \xi + W_s, Y_s, Z_s, \Gamma_s) + \frac{1}{2} \text{Trace}(\Gamma_s)) ds - \int_t^T \langle Z_s, dW_s \rangle_{\mathbb{R}^d} \quad (2)$$

and

$$Z_t = Z_0 + \int_0^t A_s ds + \int_0^t \Gamma_s dW_s. \quad (3)$$

Under suitable smoothness and regularity hypotheses the fully nonlinear PDE (1) is related to the 2BSDE system (2)–(3) in the sense that for all $t \in [0, T]$ it holds \mathbb{P} -a.s. that

$$Y_t = u(t, \xi + W_t) \in \mathbb{R}, \quad Z_t = (\nabla_x u)(t, \xi + W_t) \in \mathbb{R}^d, \quad (4)$$

$$\Gamma_t = (\text{Hess}_x u)(t, \xi + W_t) \in \mathbb{R}^{d \times d}, \quad \text{and} \quad (5)$$

$$A_t = \left(\frac{\partial}{\partial t} \nabla_x u\right)(t, \xi + W_t) + \frac{1}{2}(\nabla_x \Delta_x u)(t, \xi + W_t) \in \mathbb{R}^d \quad (6)$$

(cf., e.g., Cheridito et al. [22] and Lemma 3.1 below).

2.3 Merged formulation of the PDE and the 2BSDE

In this subsection we derive a merged formulation (see (9) and (10)) for the PDE (1) and the 2BSDE system (2)–(3). More specifically, observe that (2) and (3) yield that for all $\tau_1, \tau_2 \in [0, T]$ with $\tau_1 \leq \tau_2$ it holds \mathbb{P} -a.s. that

$$Y_{\tau_2} = Y_{\tau_1} + \int_{\tau_1}^{\tau_2} \left(f(s, \xi + W_s, Y_s, Z_s, \Gamma_s) + \frac{1}{2} \text{Trace}(\Gamma_s) \right) ds + \int_{\tau_1}^{\tau_2} \langle Z_s, dW_s \rangle_{\mathbb{R}^d} \quad (7)$$

and

$$Z_{\tau_2} = Z_{\tau_1} + \int_{\tau_1}^{\tau_2} A_s ds + \int_{\tau_1}^{\tau_2} \Gamma_s dW_s. \quad (8)$$

Putting (5) and (6) into (7) and (8) demonstrates that for all $\tau_1, \tau_2 \in [0, T]$ with $\tau_1 \leq \tau_2$ it holds \mathbb{P} -a.s. that

$$\begin{aligned} Y_{\tau_2} &= Y_{\tau_1} + \int_{\tau_1}^{\tau_2} \langle Z_s, dW_s \rangle_{\mathbb{R}^d} \\ &+ \int_{\tau_1}^{\tau_2} \left(f(s, \xi + W_s, Y_s, Z_s, (\text{Hess}_x u)(s, \xi + W_s)) + \frac{1}{2} \text{Trace}((\text{Hess}_x u)(s, \xi + W_s)) \right) ds \end{aligned} \quad (9)$$

and

$$\begin{aligned} Z_{\tau_2} &= Z_{\tau_1} + \int_{\tau_1}^{\tau_2} \left(\left(\frac{\partial}{\partial t} \nabla_x u\right)(s, \xi + W_s) + \frac{1}{2}(\nabla_x \Delta_x u)(s, \xi + W_s) \right) ds \\ &+ \int_{\tau_1}^{\tau_2} (\text{Hess}_x u)(s, \xi + W_s) dW_s. \end{aligned} \quad (10)$$

2.4 Forward-discretization of the merged PDE-2BSDE system

In this subsection we derive a forward-discretization of the merged PDE-2BSDE system (9)–(10). Let $t_0, t_1, \dots, t_N \in [0, T]$ be real numbers with

$$0 = t_0 < t_1 < \dots < t_N = T. \quad (11)$$

such that the mesh size $\sup_{0 \leq k \leq N} (t_{k+1} - t_k)$ is sufficiently small. Note that (9) and (10) suggest that for sufficiently large $N \in \mathbb{N}$ it holds for all $n \in \{0, 1, \dots, N-1\}$ that

$$\begin{aligned} Y_{t_{n+1}} &\approx Y_{t_n} + \left(f(t_n, \xi + W_{t_n}, Y_{t_n}, Z_{t_n}, (\text{Hess}_x u)(t_n, \xi + W_{t_n})) \right. \\ &\left. + \frac{1}{2} \text{Trace}((\text{Hess}_x u)(t_n, \xi + W_{t_n})) \right) (t_{n+1} - t_n) + \langle Z_{t_n}, W_{t_{n+1}} - W_{t_n} \rangle_{\mathbb{R}^d} \end{aligned} \quad (12)$$

and

$$Z_{t_{n+1}} \approx Z_{t_n} + \left(\left(\frac{\partial}{\partial t} \nabla_x u \right) (t_n, \xi + W_{t_n}) + \frac{1}{2} (\nabla_x \Delta_x u) (t_n, \xi + W_{t_n}) \right) (t_{n+1} - t_n) + (\text{Hess}_x u) (t_n, \xi + W_{t_n}) (W_{t_{n+1}} - W_{t_n}). \quad (13)$$

2.5 Deep learning approximations

In the next step we employ for every $n \in \{0, 1, \dots, N-1\}$ suitable approximations for the functions

$$\mathbb{R}^d \ni x \mapsto (\text{Hess}_x u) (t_n, x) \in \mathbb{R}^{d \times d} \quad (14)$$

and

$$\mathbb{R}^d \ni x \mapsto \left(\frac{\partial}{\partial t} \nabla_x u \right) (t_n, x) + \frac{1}{2} (\nabla_x \Delta_x u) (t_n, x) \in \mathbb{R}^d \quad (15)$$

in (12)–(13) but not for the functions $\mathbb{R}^d \ni x \mapsto u(t_n, x) \in \mathbb{R}$ and $\mathbb{R}^d \ni x \mapsto (\nabla_x u) (t_n, x) \in \mathbb{R}^d$ in (4). More precisely, let $\nu \in \mathbb{N} \cap [d+1, \infty)$, for every $\theta \in \mathbb{R}^\nu$, $n \in \{0, 1, \dots, N\}$ let $\mathbb{G}_n^\theta: \mathbb{R}^d \rightarrow \mathbb{R}^{d \times d}$ and $\mathbb{A}_n^\theta: \mathbb{R}^d \rightarrow \mathbb{R}^d$ be continuous functions, and for every $\theta = (\theta_1, \theta_2, \dots, \theta_\nu) \in \mathbb{R}^\nu$ let $\mathcal{Y}^\theta: \{0, 1, \dots, N\} \times \Omega \rightarrow \mathbb{R}$ and $\mathcal{Z}^\theta: \{0, 1, \dots, N\} \times \Omega \rightarrow \mathbb{R}^d$ be stochastic processes which satisfy that $\mathcal{Y}_0^\theta = \theta_1$ and $\mathcal{Z}_0^\theta = (\theta_2, \theta_3, \dots, \theta_{d+1})$ and which satisfy for all $n \in \{0, 1, \dots, N-1\}$ that

$$\begin{aligned} \mathcal{Y}_{n+1}^\theta &= \mathcal{Y}_n^\theta + \langle \mathcal{Z}_n^\theta, W_{t_{n+1}} - W_{t_n} \rangle_{\mathbb{R}^d} \\ &+ \left(f(t_n, \xi + W_{t_n}, \mathcal{Y}_n^\theta, \mathcal{Z}_n^\theta, \mathbb{G}_n^\theta(\xi + W_{t_n})) + \frac{1}{2} \text{Trace}(\mathbb{G}_n^\theta(\xi + W_{t_n})) \right) (t_{n+1} - t_n) \end{aligned} \quad (16)$$

and

$$\mathcal{Z}_{n+1}^\theta = \mathcal{Z}_n^\theta + \mathbb{A}_n^\theta(\xi + W_{t_n}) (t_{n+1} - t_n) + \mathbb{G}_n^\theta(\xi + W_{t_n}) (W_{t_{n+1}} - W_{t_n}). \quad (17)$$

For all suitable $\theta \in \mathbb{R}^\nu$ and all $n \in \{0, 1, \dots, N\}$ we think of $\mathcal{Y}_n^\theta: \Omega \rightarrow \mathbb{R}$ as an appropriate approximation

$$\mathcal{Y}_n^\theta \approx Y_{t_n} \quad (18)$$

of $Y_{t_n}: \Omega \rightarrow \mathbb{R}$, for all suitable $\theta \in \mathbb{R}^\nu$ and all $n \in \{0, 1, \dots, N\}$ we think of $\mathcal{Z}_n^\theta: \Omega \rightarrow \mathbb{R}^d$ as an appropriate approximation

$$\mathcal{Z}_n^\theta \approx Z_{t_n} \quad (19)$$

of $Z_{t_n}: \Omega \rightarrow \mathbb{R}^d$, for all suitable $\theta \in \mathbb{R}^\nu$, $x \in \mathbb{R}^d$ and all $n \in \{0, 1, \dots, N-1\}$ we think of $\mathbb{G}_n^\theta(x) \in \mathbb{R}^{d \times d}$ as an appropriate approximation

$$\mathbb{G}_n^\theta(x) \approx (\text{Hess}_x u) (t_n, x) \quad (20)$$

of $(\text{Hess}_x u) (t_n, x) \in \mathbb{R}^{d \times d}$, and for all suitable $\theta \in \mathbb{R}^\nu$, $x \in \mathbb{R}^d$ and all $n \in \{0, 1, \dots, N-1\}$ we think of $\mathbb{A}_n^\theta(x) \in \mathbb{R}^d$ as an appropriate approximation

$$\mathbb{A}_n^\theta(x) \approx \left(\frac{\partial}{\partial t} \nabla_x u \right) (t_n, x) + \frac{1}{2} (\nabla_x \Delta_x u) (t_n, x) \quad (21)$$

of $(\frac{\partial}{\partial t} \nabla_x u)(t_n, x) + \frac{1}{2}(\nabla_x \Delta_x u)(t_n, x) \in \mathbb{R}^d$. In particular, we think of θ_1 as an appropriate approximation

$$\theta_1 \approx u(0, \xi) \quad (22)$$

of $u(0, \xi) \in \mathbb{R}$, and we think of $(\theta_2, \theta_3, \dots, \theta_{d+1})$ as an appropriate approximation

$$(\theta_2, \theta_3, \dots, \theta_{d+1}) \approx (\nabla_x u)(0, \xi) \quad (23)$$

of $(\nabla_x u)(0, \xi) \in \mathbb{R}^d$. We suggest for every $n \in \{0, 1, \dots, N-1\}$ to choose the functions \mathbb{G}_n^θ and \mathbb{A}_n^θ as deep neural networks (cf., e.g., [8, 67]). For example, for every $k \in \mathbb{N}$ let $\mathcal{R}_k: \mathbb{R}^k \rightarrow \mathbb{R}^k$ be the function which satisfies for all $x = (x_1, \dots, x_k) \in \mathbb{R}^k$ that

$$\mathcal{R}_k(x) = (\max\{x_1, 0\}, \dots, \max\{x_k, 0\}), \quad (24)$$

for every $\theta = (\theta_1, \dots, \theta_\nu) \in \mathbb{R}^\nu$, $v \in \mathbb{N}_0 = \{0\} \cup \mathbb{N}$, $k, l \in \mathbb{N}$ with $v + k(l+1) \leq \nu$ let $M_{k,l}^{\theta,v}: \mathbb{R}^l \rightarrow \mathbb{R}^k$ be the affine linear function which satisfies for all $x = (x_1, \dots, x_l)$ that

$$M_{k,l}^{\theta,v}(x) = \begin{pmatrix} \theta_{v+1} & \theta_{v+2} & \dots & \theta_{v+l} \\ \theta_{v+l+1} & \theta_{v+l+2} & \dots & \theta_{v+2l} \\ \theta_{v+2l+1} & \theta_{v+2l+2} & \dots & \theta_{v+3l} \\ \vdots & \vdots & \vdots & \vdots \\ \theta_{v+(k-1)l+1} & \theta_{v+(k-1)l+2} & \dots & \theta_{v+kl} \end{pmatrix} \begin{pmatrix} x_1 \\ x_2 \\ x_3 \\ \vdots \\ x_l \end{pmatrix} + \begin{pmatrix} \theta_{v+kl+1} \\ \theta_{v+kl+2} \\ \theta_{v+kl+3} \\ \vdots \\ \theta_{v+kl+k} \end{pmatrix}, \quad (25)$$

assume that $\nu \geq (5Nd + Nd^2 + 1)(d+1)$, and assume for all $\theta \in \mathbb{R}^\nu$, $n \in \{m \in \mathbb{N}: m < N\}$, $x \in \mathbb{R}^d$ that

$$\mathbb{A}_n^\theta = M_{d,d}^{\theta, [(2N+n)d+1](d+1)} \circ \mathcal{R}_d \circ M_{d,d}^{\theta, [(N+n)d+1](d+1)} \circ \mathcal{R}_d \circ M_{d,d}^{\theta, (nd+1)(d+1)} \quad (26)$$

and

$$\mathbb{G}_n^\theta = M_{d^2,d}^{\theta, (5Nd+nd^2+1)(d+1)} \circ \mathcal{R}_d \circ M_{d,d}^{\theta, [(4N+n)d+1](d+1)} \circ \mathcal{R}_d \circ M_{d,d}^{\theta, [(3N+n)d+1](d+1)}. \quad (27)$$

The functions in (26) provide artificial neural networks with 4 layers (1 input layer with d neurons, 2 hidden layers with d neurons each, and 1 output layer with d neurons) and rectifier functions as activation functions (see (24)). The functions in (27) also provide artificial neural networks with 4 layers (1 input layer with d neurons, 2 hidden layers with d neurons each, and 1 output layer with d^2 neurons) and rectifier functions as activation functions (see (24)).

2.6 Stochastic gradient descent-type optimization

We intend to reach a *suitable* $\theta \in \mathbb{R}^\nu$ in (18)–(23) by applying a stochastic gradient descent-type minimization algorithm to the function

$$\mathbb{R}^\nu \ni \theta \mapsto \mathbb{E}[|\mathcal{Y}_N^\theta - g(\xi + W_{t_N})|^2] \in \mathbb{R}. \quad (28)$$

Minimizing the function in (28) is inspired by the fact that

$$\mathbb{E}[|Y_T - g(\xi + W_T)|^2] = 0 \quad (29)$$

according to (2). Applying a stochastic gradient descent-type minimization algorithm yields under suitable assumptions random approximations

$$\Theta_m = (\Theta_m^{(1)}, \Theta_m^{(2)}, \dots, \Theta_m^{(\nu)}): \Omega \rightarrow \mathbb{R}^\nu \quad (30)$$

for $m \in \mathbb{N}_0$ of a local minimum point of the function in (28). For sufficiently large $N, \nu, m \in \mathbb{N}$ we use the random variable $\Theta_m^{(1)}: \Omega \rightarrow \mathbb{R}$ as an appropriate approximation

$$\Theta_m^{(1)} \approx u(0, \xi) \quad (31)$$

of $u(0, \xi) \in \mathbb{R}$ (cf. (22) above). In the next subsection the proposed algorithm is described in more detail.

2.7 Framework for the algorithm in a specific case

In this subsection we describe the deep 2BSDE method in the specific case where (1) is the PDE under consideration, where the standard Euler-Maruyama scheme (cf., e.g., [61, 76, 80]) is the employed approximation scheme for discretizing (9) and (10) (cf. (16) and (17)), and where the plain stochastic gradient descent with constant learning rate $\gamma \in (0, \infty)$ is the employed minimization algorithm. A more general description of the deep 2BSDE method, which allows to incorporate more sophisticated machine learning approximation techniques such as batch normalization or the Adam optimizer, can be found in Subsection 3.7 below.

Framework 2.1 (Special case). *Let $T, \gamma \in (0, \infty)$, $d, N \in \mathbb{N}$, $\nu \in \mathbb{N} \cap [d+1, \infty)$, $\xi \in \mathbb{R}^d$, let $f: [0, T] \times \mathbb{R}^d \times \mathbb{R} \times \mathbb{R}^d \times \mathbb{R}^{d \times d} \rightarrow \mathbb{R}$ and $g: \mathbb{R}^d \rightarrow \mathbb{R}$ be functions, let $(\Omega, \mathcal{F}, \mathbb{P})$ be a probability space, let $W^m: [0, T] \times \Omega \rightarrow \mathbb{R}^d$, $m \in \mathbb{N}_0$, be independent standard Brownian motions on $(\Omega, \mathcal{F}, \mathbb{P})$, let $t_0, t_1, \dots, t_N \in [0, T]$ be real numbers with $0 = t_0 < t_1 < \dots < t_N = T$, for every $\theta \in \mathbb{R}^\nu$, $n \in \{0, 1, \dots, N-1\}$ let $\mathbb{A}_n^\theta: \mathbb{R}^d \rightarrow \mathbb{R}^d$ and $\mathbb{G}_n^\theta: \mathbb{R}^d \rightarrow \mathbb{R}^{d \times d}$ be functions, for every $m \in \mathbb{N}_0$, $\theta \in \mathbb{R}^\nu$ let $\mathcal{Y}^{m, \theta}: \{0, 1, \dots, N\} \times \Omega \rightarrow \mathbb{R}$ and $\mathcal{Z}^{m, \theta}: \{0, 1, \dots, N\} \times \Omega \rightarrow \mathbb{R}^d$ be stochastic processes which satisfy that $\mathcal{Y}_0^{m, \theta} = \theta_1$ and $\mathcal{Z}_0^{m, \theta} = (\theta_2, \theta_3, \dots, \theta_{d+1})$ and which satisfy for all $n \in \{0, 1, \dots, N-1\}$ that*

$$\begin{aligned} \mathcal{Y}_{n+1}^{m, \theta} &= \mathcal{Y}_n^{m, \theta} + \langle \mathcal{Z}_n^{m, \theta}, W_{t_{n+1}}^m - W_{t_n}^m \rangle_{\mathbb{R}^d} \\ &+ \left(f(t_n, \xi + W_{t_n}^m, \mathcal{Y}_n^{m, \theta}, \mathcal{Z}_n^{m, \theta}, \mathbb{G}_n^\theta(\xi + W_{t_n}^m)) + \frac{1}{2} \text{Trace}(\mathbb{G}_n^\theta(\xi + W_{t_n}^m)) \right) (t_{n+1} - t_n) \end{aligned} \quad (32)$$

$$\text{and} \quad \mathcal{Z}_{n+1}^{m, \theta} = \mathcal{Z}_n^{m, \theta} + \mathbb{A}_n^\theta(\xi + W_{t_n}^m) (t_{n+1} - t_n) + \mathbb{G}_n^\theta(\xi + W_{t_n}^m) (W_{t_{n+1}}^m - W_{t_n}^m), \quad (33)$$

for every $m \in \mathbb{N}_0$ let $\phi^m: \mathbb{R}^\nu \times \Omega \rightarrow \mathbb{R}$ be the function which satisfies for all $\theta \in \mathbb{R}^\nu$, $\omega \in \Omega$ that

$$\phi^m(\theta, \omega) = |\mathcal{Y}_N^{m, \theta}(\omega) - g(\xi + W_T^m(\omega))|^2, \quad (34)$$

for every $m \in \mathbb{N}_0$ let $\Phi^m: \mathbb{R}^\nu \times \Omega \rightarrow \mathbb{R}^\nu$ be a function which satisfies for all $\omega \in \Omega$, $\theta \in \{\eta \in \mathbb{R}^\nu: \phi^m(\cdot, \omega): \mathbb{R}^\nu \rightarrow \mathbb{R} \text{ is differentiable at } \eta\}$ that

$$\Phi^m(\theta, \omega) = (\nabla_\theta \phi^m)(\theta, \omega), \quad (35)$$

and let $\Theta = (\Theta^{(1)}, \dots, \Theta^{(\nu)}): \mathbb{N}_0 \times \Omega \rightarrow \mathbb{R}^\nu$ be a stochastic process which satisfies for all $m \in \mathbb{N}_0$ that

$$\Theta_{m+1} = \Theta_m - \gamma \cdot \Phi^m(\Theta_m). \quad (36)$$

Under suitable further assumptions, we think in the case of sufficiently large $N, \nu \in \mathbb{N}$, $m \in \mathbb{N}_0$ and sufficiently small $\gamma \in (0, \infty)$ in Framework 2.1 of the random variable $\Theta_m = (\Theta_m^{(1)}, \dots, \Theta_m^{(\nu)}): \Omega \rightarrow \mathbb{R}^\nu$ as an appropriate approximation of a local minimum point of the expected loss function and we think in the case of sufficiently large $N, \nu \in \mathbb{N}$, $m \in \mathbb{N}_0$ and sufficiently small $\gamma \in (0, \infty)$ in Framework 2.1 of the random variable $\Theta_m^{(1)}: \Omega \rightarrow \mathbb{R}$ as an appropriate approximation of the value $u(0, \xi) \in \mathbb{R}$ where $u: [0, T] \times \mathbb{R}^d \rightarrow \mathbb{R}$ is an at most polynomially growing continuous function which satisfies for all $(t, x) \in [0, T) \times \mathbb{R}^d$ that $u|_{[0, T) \times \mathbb{R}^d} \in C^{1,2}([0, T) \times \mathbb{R}^d, \mathbb{R})$, $u(T, x) = g(x)$, and

$$\frac{\partial u}{\partial t}(t, x) = f(t, x, u(t, x), (\nabla_x u)(t, x), (\text{Hess}_x u)(t, x)). \quad (37)$$

In Subsection 4.1 below an implementation of Framework 2.1 (see PYTHON code 1 in Appendix A.1 below) is employed to calculate numerical approximations for the Allen-Cahn equation in 20 space-dimensions ($d = 20$). In Subsection 4.5 below numerical approximations for the Allen-Cahn equation in 50 space-dimensions are calculated by means of the algorithm in the more general setting in Framework 3.2 below.

3 The deep 2BSDE method in the general case

In this section we extend and generalize the approximation scheme derived and presented in Section 2. The core idea of the approximation scheme in this section remains the same as in Section 2 but, in contrast to Section 2, in this section the background dynamics in the approximation scheme may be a more general Itô process than just a Brownian motion (cf. Lemma 3.1 in Subsection 3.2 below) and, in contrast to Section 2, in this section the approximation scheme may employ more sophisticated machine learning techniques (cf. Framework 3.2 in Subsection 3.7 below).

3.1 Fully nonlinear second-order PDEs

Let $d \in \mathbb{N}$, $T \in (0, \infty)$, let $u = (u(t, x))_{t \in [0, T], x \in \mathbb{R}^d} \in C^{1,2}([0, T] \times \mathbb{R}^d, \mathbb{R})$, $f: [0, T] \times \mathbb{R}^d \times \mathbb{R} \times \mathbb{R}^d \times \mathbb{R}^{d \times d} \rightarrow \mathbb{R}$, and $g: [0, T] \times \mathbb{R}^d \rightarrow \mathbb{R}$ be functions which satisfy for all $(t, x) \in [0, T] \times \mathbb{R}^d$ that $u(T, x) = g(x)$ and

$$\frac{\partial u}{\partial t}(t, x) = f(t, x, u(t, x), (\nabla_x u)(t, x), (\text{Hess}_x u)(t, x)). \quad (38)$$

Our goal is to approximatively compute the solution u of the PDE (38) at time $t = 0$, that is, our goal is to approximatively calculate the function $\mathbb{R}^d \ni x \mapsto u(0, x) \in \mathbb{R}$. For this, we make use of the following connection between fully nonlinear second-order PDEs and second-order BSDEs.

3.2 Connection between fully nonlinear second-order PDEs and 2BSDEs

The deep 2BSDE method relies on a connection between fully nonlinear second-order PDEs and second-order BSDEs; cf., e.g., Theorem 4.10 in Cheridito et al. [22] and Lemma 3.1 below.

Lemma 3.1 (Cf., e.g., Section 3 in Cheridito et al. [22]). *Let $d \in \mathbb{N}$, $T \in (0, \infty)$, let $u = (u(t, x))_{t \in [0, T], x \in \mathbb{R}^d} \in C^{1,2}([0, T] \times \mathbb{R}^d, \mathbb{R})$, $\mu \in C(\mathbb{R}^d, \mathbb{R}^d)$, $\sigma \in C(\mathbb{R}^d, \mathbb{R}^{d \times d})$, $f: [0, T] \times \mathbb{R}^d \times \mathbb{R} \times \mathbb{R}^d \times \mathbb{R}^{d \times d} \rightarrow \mathbb{R}$, and $g: \mathbb{R}^d \rightarrow \mathbb{R}$ be functions which satisfy for all $t \in [0, T]$, $x \in \mathbb{R}^d$ that $\nabla_x u \in C^{1,2}([0, T] \times \mathbb{R}^d, \mathbb{R}^d)$, $u(T, x) = g(x)$, and*

$$\frac{\partial u}{\partial t}(t, x) = f(t, x, u(t, x), (\nabla_x u)(t, x), (\text{Hess}_x u)(t, x)), \quad (39)$$

let $(\Omega, \mathcal{F}, \mathbb{P})$ be a probability space, let $W = (W^{(1)}, \dots, W^{(d)}): [0, T] \times \Omega \rightarrow \mathbb{R}^d$ be a standard Brownian motion on $(\Omega, \mathcal{F}, \mathbb{P})$, let $\mathbb{F} = (\mathbb{F}_t)_{t \in [0, T]}$ be the normal filtration on $(\Omega, \mathcal{F}, \mathbb{P})$ generated by W , let $\xi: \Omega \rightarrow \mathbb{R}^d$ be an $\mathcal{F}_0/\mathcal{B}(\mathbb{R}^d)$ -measurable function, let $X = (X^{(1)}, \dots, X^{(d)}): [0, T] \times \Omega \rightarrow \mathbb{R}^d$ be an \mathbb{F} -adapted stochastic process with continuous sample paths which satisfies that for all $t \in [0, T]$ it holds \mathbb{P} -a.s. that

$$X_t = \xi + \int_0^t \mu(X_s) ds + \int_0^t \sigma(X_s) dW_s, \quad (40)$$

for every $\varphi \in C^{1,2}([0, T] \times \mathbb{R}^d, \mathbb{R})$ let $\mathcal{L}\varphi: [0, T] \times \mathbb{R}^d \rightarrow \mathbb{R}$ be the function which satisfies for all $(t, x) \in [0, T] \times \mathbb{R}^d$ that

$$(\mathcal{L}\varphi)(t, x) = \left(\frac{\partial \varphi}{\partial t}\right)(t, x) + \frac{1}{2} \text{Trace}(\sigma(x)\sigma(x)^*(\text{Hess}_x \varphi)(t, x)), \quad (41)$$

and let $Y: [0, T] \times \Omega \rightarrow \mathbb{R}$, $Z = (Z^{(1)}, \dots, Z^{(d)}): [0, T] \times \Omega \rightarrow \mathbb{R}^d$, $\Gamma = (\Gamma^{(i,j)})_{(i,j) \in \{1, \dots, d\}^2}: [0, T] \times \Omega \rightarrow \mathbb{R}^{d \times d}$, and $A = (A^{(1)}, \dots, A^{(d)}): [0, T] \times \Omega \rightarrow \mathbb{R}^d$ be the stochastic processes which satisfy for all $t \in [0, T]$, $i \in \{1, 2, \dots, d\}$ that

$$Y_t = u(t, X_t), \quad Z_t = (\nabla_x u)(t, X_t), \quad \Gamma_t = (\text{Hess}_x u)(t, X_t), \quad A_t^{(i)} = (\mathcal{L}(\frac{\partial u}{\partial x_i}))(t, X_t). \quad (42)$$

Then it holds that Y , Z , Γ , and A are \mathbb{F} -adapted stochastic processes with continuous sample paths which satisfy that for all $t \in [0, T]$ it holds \mathbb{P} -a.s. that

$$Y_t = g(X_T) - \int_t^T \left(f(s, X_s, Y_s, Z_s, \Gamma_s) + \frac{1}{2} \text{Trace}(\sigma(X_s)\sigma(X_s)^*\Gamma_s) \right) ds - \int_t^T \langle Z_s, dX_s \rangle_{\mathbb{R}^d} \quad (43)$$

and

$$Z_t = Z_0 + \int_0^t A_s ds + \int_0^t \Gamma_s dX_s. \quad (44)$$

Proof of Lemma 3.1. Note that $u: [0, T] \times \mathbb{R}^d \rightarrow \mathbb{R}$, $\nabla_x u: [0, T] \times \mathbb{R}^d \rightarrow \mathbb{R}^d$, $\text{Hess}_x u: [0, T] \times \mathbb{R}^d \rightarrow \mathbb{R}^{d \times d}$, and $(\mathcal{L} \frac{\partial u}{\partial x_i}): [0, T] \times \mathbb{R}^d \rightarrow \mathbb{R}$, $i \in \{1, 2, \dots, d\}$, are continuous functions. Combining this and (42) with the continuity of the sample paths of X shows that Y , Z , Γ , and A are \mathbb{F} -adapted stochastic process with continuous sample paths. Next observe that Itô's lemma and the assumption that $u \in C^{1,2}([0, T] \times \mathbb{R}^d, \mathbb{R})$ yield that for all $r \in [0, T]$ it holds \mathbb{P} -a.s. that

$$\begin{aligned} u(T, X_T) &= u(r, X_r) + \int_r^T \langle (\nabla_x u)(s, X_s), dX_s \rangle_{\mathbb{R}^d} \\ &\quad + \int_r^T \left(\left(\frac{\partial u}{\partial t} \right)(s, X_s) + \frac{1}{2} \text{Trace}(\sigma(X_s)\sigma(X_s)^*(\text{Hess}_x u)(s, X_s)) \right) ds. \end{aligned} \quad (45)$$

This, (39), and (42) yield that for all $r \in [0, T]$ it holds \mathbb{P} -a.s. that

$$\begin{aligned} g(X_T) &= Y_r + \int_r^T \langle Z_s, dX_s \rangle_{\mathbb{R}^d} \\ &\quad + \int_r^T \left(f(s, X_s, Y_s, Z_s, \Gamma_s) + \frac{1}{2} \text{Trace}(\sigma(X_s)\sigma(X_s)^*\Gamma_s) \right) ds. \end{aligned} \quad (46)$$

This establishes (43). In the next step we note that Itô's lemma and the hypothesis that $\nabla_x u = (\frac{\partial u}{\partial x_1}, \dots, \frac{\partial u}{\partial x_d}) \in C^{1,2}([0, T] \times \mathbb{R}^d, \mathbb{R}^d)$ guarantee that for all $i \in \{1, 2, \dots, d\}$, $r \in [0, T]$ it holds \mathbb{P} -a.s. that

$$\begin{aligned} \left(\frac{\partial u}{\partial x_i} \right)(r, X_r) &= \left(\frac{\partial u}{\partial x_i} \right)(0, X_0) + \int_0^r \langle (\nabla_x \frac{\partial u}{\partial x_i})(s, X_s), dX_s \rangle_{\mathbb{R}^d} \\ &\quad + \int_0^r \left(\left(\frac{\partial}{\partial t} \frac{\partial u}{\partial x_i} \right)(s, X_s) + \frac{1}{2} \text{Trace}(\sigma(X_s)\sigma(X_s)^*(\text{Hess}_x \frac{\partial u}{\partial x_i})(s, X_s)) \right) ds. \end{aligned} \quad (47)$$

This, (41), and (42) yield that for all $i \in \{1, 2, \dots, d\}$, $r \in [0, T]$ it holds \mathbb{P} -a.s. that

$$\begin{aligned} Z_r^{(i)} &= Z_0^{(i)} + \sum_{j=1}^d \int_0^r \left(\frac{\partial}{\partial x_j} \frac{\partial u}{\partial x_i} \right)(s, X_s) dX_s^{(j)} \\ &\quad + \int_0^r \left(\left(\frac{\partial}{\partial t} \frac{\partial u}{\partial x_i} \right)(s, X_s) + \frac{1}{2} \text{Trace}(\sigma(X_s) \sigma(X_s)^* (\text{Hess}_x \frac{\partial u}{\partial x_i})(s, X_s)) \right) ds \quad (48) \\ &= Z_0^{(i)} + \int_0^r A_s^{(i)} ds + \sum_{j=1}^d \int_0^r \Gamma_s^{(i,j)} dX_s^{(j)}. \end{aligned}$$

This shows (44). The proof of Lemma 3.1 is thus completed. \square

In Subsection 2.2 above we have employed Lemma 3.1 in the specific situation where $\forall x \in \mathbb{R}^d: \mu(x) = 0 \in \mathbb{R}^d$ and $\forall x \in \mathbb{R}^d: \sigma(x) = \text{Id}_{\mathbb{R}^d} \in \mathbb{R}^{d \times d}$ (cf. (2)–(6) in Subsection 2.2 and (43)–(44) in Lemma 3.1). In the following we proceed with the merged formulation, the forward-discretization of the merged PDE-2BSDE system, and deep learning approximations similar as in Section 2.

3.3 Merged formulation of the PDE and the 2BSDE

In this subsection we derive a merged formulation (see (55) and (56)) for the PDE (38) and the 2BSDE system (53)–(54) as in Subsection 2.3. To derive the merged formulation of the PDE and the 2BSDE, we employ the following hypotheses in addition to the assumptions in Subsection 3.1 above (cf. Lemma 3.1 above). Let $\mu: \mathbb{R}^d \rightarrow \mathbb{R}^d$ and $\sigma: \mathbb{R}^d \rightarrow \mathbb{R}^{d \times d}$ be continuous functions, let $(\Omega, \mathcal{F}, \mathbb{P})$ be a probability space, let $W: [0, T] \times \Omega \rightarrow \mathbb{R}^d$ be a standard Brownian motion on $(\Omega, \mathcal{F}, \mathbb{P})$, let $\mathbb{F} = (\mathbb{F}_t)_{t \in [0, T]}$ be the normal filtration on $(\Omega, \mathcal{F}, \mathbb{P})$ generated by W , let $\xi: \Omega \rightarrow \mathbb{R}^d$ be an $\mathcal{F}_0/\mathcal{B}(\mathbb{R}^d)$ -measurable function, let $X = (X^{(1)}, \dots, X^{(d)}): [0, T] \times \Omega \rightarrow \mathbb{R}^d$ be an \mathbb{F} -adapted stochastic process with continuous sample paths which satisfies that for all $t \in [0, T]$ it holds \mathbb{P} -a.s. that

$$X_t = \xi + \int_0^t \mu(X_s) ds + \int_0^t \sigma(X_s) dW_s, \quad (49)$$

let $e_1^{(d)} = (1, 0, \dots, 0)$, $e_2^{(d)} = (0, 1, 0, \dots, 0)$, \dots , $e_d^{(d)} = (0, \dots, 0, 1) \in \mathbb{R}^d$ be the standard basis vectors of \mathbb{R}^d , for every $\varphi \in C^{1,2}([0, T] \times \mathbb{R}^d, \mathbb{R}^d)$ let $\mathcal{L}\varphi: [0, T] \times \mathbb{R}^d \rightarrow \mathbb{R}^d$ be the function which satisfies for all $(t, x) \in [0, T] \times \mathbb{R}^d$ that

$$(\mathcal{L}\varphi)(t, x) = \frac{\partial \varphi}{\partial t}(t, x) + \frac{1}{2} \sum_{i=1}^d \left(\frac{\partial^2 \varphi}{\partial x^2} \right)(t, x) (\sigma(x) e_i^{(d)}, \sigma(x) e_i^{(d)}) \quad (50)$$

and let $Y: [0, T] \times \Omega \rightarrow \mathbb{R}$, $Z: [0, T] \times \Omega \rightarrow \mathbb{R}^d$, $\Gamma: [0, T] \times \Omega \rightarrow \mathbb{R}^{d \times d}$, and $A: [0, T] \times \Omega \rightarrow \mathbb{R}^d$ be the stochastic processes which satisfy for all $t \in [0, T]$ that

$$Y_t = u(t, X_t), \quad Z_t = (\nabla_x u)(t, X_t), \quad \Gamma_t = (\text{Hess}_x u)(t, X_t), \quad A_t = (\mathcal{L}(\nabla_x u))(t, X_t). \quad (51)$$

Lemma 3.1 implies that for all $\tau_1, \tau_2 \in [0, T]$ with $\tau_1 \leq \tau_2$ it holds \mathbb{P} -a.s. that

$$X_{\tau_2} = X_{\tau_1} + \int_{\tau_1}^{\tau_2} \mu(X_s) ds + \int_{\tau_1}^{\tau_2} \sigma(X_s) dW_s, \quad (52)$$

$$Y_{\tau_2} = Y_{\tau_1} + \int_{\tau_1}^{\tau_2} \left(f(s, X_s, Y_s, Z_s, \Gamma_s) + \frac{1}{2} \text{Trace}(\sigma(X_s) \sigma(X_s)^* \Gamma_s) \right) ds + \int_{\tau_1}^{\tau_2} \langle Z_s, dX_s \rangle_{\mathbb{R}^d}, \quad (53)$$

and

$$Z_{\tau_2} = Z_{\tau_1} + \int_{\tau_1}^{\tau_2} A_s ds + \int_{\tau_1}^{\tau_2} \Gamma_s dX_s. \quad (54)$$

Putting the third and the fourth identity in (51) into (53) and (54) yields that for all $\tau_1, \tau_2 \in [0, T]$ with $\tau_1 \leq \tau_2$ it holds \mathbb{P} -a.s. that

$$\begin{aligned} Y_{\tau_2} &= Y_{\tau_1} + \int_{\tau_1}^{\tau_2} \langle Z_s, dX_s \rangle_{\mathbb{R}^d} \\ &+ \int_{\tau_1}^{\tau_2} \left(f(s, X_s, Y_s, Z_s, (\text{Hess}_x u)(s, X_s)) + \frac{1}{2} \text{Trace}(\sigma(X_s) \sigma(X_s)^* (\text{Hess}_x u)(s, X_s)) \right) ds \end{aligned} \quad (55)$$

and

$$Z_{\tau_2} = Z_{\tau_1} + \int_{\tau_1}^{\tau_2} (\mathcal{L}(\nabla_x u))(s, X_s) ds + \int_{\tau_1}^{\tau_2} (\text{Hess}_x u)(s, X_s) dX_s. \quad (56)$$

3.4 Forward-discretization of the merged PDE-2BSDE system

In this subsection we derive a forward-discretization of the merged PDE-2BSDE system (55)–(56) (cf. Subsection 2.4). Let $t_0, t_1, \dots, t_N \in [0, T]$ be real numbers with

$$0 = t_0 < t_1 < \dots < t_N = T \quad (57)$$

such that the small mesh size $\sup_{0 \leq k \leq N} (t_{k+1} - t_k)$ is sufficiently small. Note that (51), (52), (55), and (56) suggest that for sufficiently large $N \in \mathbb{N}$ it holds for all $n \in \{0, 1, \dots, N-1\}$ that

$$X_{t_0} = X_0 = \xi, \quad Y_{t_0} = Y_0 = u(0, \xi), \quad Z_{t_0} = Z_0 = (\nabla_x u)(0, \xi), \quad (58)$$

$$X_{t_{n+1}} \approx X_{t_n} + \mu(X_{t_n})(t_{n+1} - t_n) + \sigma(X_{t_n})(X_{t_{n+1}} - X_{t_n}), \quad (59)$$

$$\begin{aligned} Y_{t_{n+1}} &\approx Y_{t_n} + \left(f(t_n, X_{t_n}, Y_{t_n}, Z_{t_n}, (\text{Hess}_x u)(t_n, X_{t_n})) \right. \\ &\left. + \frac{1}{2} \text{Trace}(\sigma(X_{t_n}) \sigma(X_{t_n})^* (\text{Hess}_x u)(t_n, X_{t_n})) \right) (t_{n+1} - t_n) + \langle Z_{t_n}, X_{t_{n+1}} - X_{t_n} \rangle_{\mathbb{R}^d}, \end{aligned} \quad (60)$$

and

$$Z_{t_{n+1}} \approx Z_{t_n} + (\mathcal{L}(\nabla_x u))(t_n, X_{t_n})(t_{n+1} - t_n) + (\text{Hess}_x u)(t_n, X_{t_n})(X_{t_{n+1}} - X_{t_n}) \quad (61)$$

(cf. (12)–(13) in Subsection 2.4 above).

3.5 Deep learning approximations

In the next step we employ suitable approximations for the functions

$$\mathbb{R}^d \ni x \mapsto u(0, x) \in \mathbb{R} \quad \text{and} \quad \mathbb{R}^d \ni x \mapsto (\nabla_x u)(0, x) \in \mathbb{R}^d \quad (62)$$

in (58) and we employ for every $n \in \{0, 1, \dots, N-1\}$ suitable approximations for the functions

$$\mathbb{R}^d \ni x \mapsto (\text{Hess}_x u)(t_n, x) \in \mathbb{R}^{d \times d} \quad \text{and} \quad \mathbb{R}^d \ni x \mapsto (\mathcal{L}(\nabla_x u))(t_n, x) \in \mathbb{R}^d \quad (63)$$

in (60)–(61). However, we do neither employ approximations for the functions $\mathbb{R}^d \ni x \mapsto u(t_n, x) \in \mathbb{R}$, $n \in \{1, 2, \dots, N-1\}$, nor for the functions $\mathbb{R}^d \ni x \mapsto (\nabla_x u)(t_n, x) \in \mathbb{R}^d$, $n \in \{1, 2, \dots, N-1\}$. More formally, let $\mathcal{X}: \{0, 1, \dots, N\} \times \Omega \rightarrow \mathbb{R}^d$ be a stochastic process which satisfies for all $n \in \{0, 1, \dots, N-1\}$ that $\mathcal{X}_0 = \xi$ and

$$\mathcal{X}_{n+1} = \mathcal{X}_n + \mu(\mathcal{X}_n)(t_{n+1} - t_n) + \sigma(\mathcal{X}_n)(\mathcal{X}_{n+1} - \mathcal{X}_n), \quad (64)$$

let $\nu \in \mathbb{N}$, for every $\theta \in \mathbb{R}^\nu$ let $\mathbb{U}^\theta: \mathbb{R}^d \rightarrow \mathbb{R}$ and $\mathbb{Z}^\theta: \mathbb{R}^d \rightarrow \mathbb{R}^d$ be continuous functions, for every $\theta \in \mathbb{R}^\nu$, $n \in \{0, 1, \dots, N-1\}$ let $\mathbb{G}_n^\theta: \mathbb{R}^d \rightarrow \mathbb{R}^{d \times d}$ and $\mathbb{A}_n^\theta: \mathbb{R}^d \rightarrow \mathbb{R}^d$ be continuous functions, and for every $\theta = (\theta_1, \dots, \theta_\nu) \in \mathbb{R}^\nu$ let $\mathcal{Y}^\theta: \{0, 1, \dots, N\} \times \Omega \rightarrow \mathbb{R}$ and $\mathcal{Z}^\theta: \{0, 1, \dots, N\} \times \Omega \rightarrow \mathbb{R}^d$ be stochastic processes which satisfy $\mathcal{Y}_0^\theta = \mathbb{U}^\theta(\xi)$ and $\mathcal{Z}_0^\theta = \mathbb{Z}^\theta(\xi)$ and which satisfy for all $n \in \{0, 1, \dots, N-1\}$ that

$$\begin{aligned} \mathcal{Y}_{n+1}^\theta &= \mathcal{Y}_n^\theta + \langle \mathcal{Z}_n^\theta, \mathcal{X}_{t_{n+1}} - \mathcal{X}_{t_n} \rangle_{\mathbb{R}^d} \\ &+ \left(f(t_n, \mathcal{X}_n, \mathcal{Y}_n^\theta, \mathcal{Z}_n^\theta, \mathbb{G}_n^\theta(\mathcal{X}_n)) + \frac{1}{2} \text{Trace}(\sigma(\mathcal{X}_n)\sigma(\mathcal{X}_n)^*\mathbb{G}_n^\theta(\mathcal{X}_n)) \right) (t_{n+1} - t_n) \end{aligned} \quad (65)$$

and

$$\mathcal{Z}_{n+1}^\theta = \mathcal{Z}_n^\theta + \mathbb{A}_n^\theta(\mathcal{X}_n)(t_{n+1} - t_n) + \mathbb{G}_n^\theta(\mathcal{X}_n)(\mathcal{X}_{n+1} - \mathcal{X}_n). \quad (66)$$

For all suitable $\theta \in \mathbb{R}^\nu$ and all $n \in \{0, 1, \dots, N\}$ we think of $\mathcal{Y}_n^\theta: \Omega \rightarrow \mathbb{R}$ as an appropriate approximation

$$\mathcal{Y}_n^\theta \approx Y_{t_n} \quad (67)$$

of $Y_{t_n}: \Omega \rightarrow \mathbb{R}$, for all suitable $\theta \in \mathbb{R}^\nu$ and all $n \in \{0, 1, \dots, N\}$ we think of $\mathcal{Z}_n^\theta: \Omega \rightarrow \mathbb{R}^d$ as an appropriate approximation

$$\mathcal{Z}_n^\theta \approx Z_{t_n} \quad (68)$$

of $Z_{t_n}: \Omega \rightarrow \mathbb{R}^d$, for all suitable $\theta \in \mathbb{R}^\nu$, $x \in \mathbb{R}^d$ we think of $\mathbb{U}^\theta(x) \in \mathbb{R}$ as an appropriate approximation

$$\mathbb{U}^\theta(x) \approx u(0, x) \quad (69)$$

of $u(0, x) \in \mathbb{R}$, for all suitable $\theta \in \mathbb{R}^\nu$, $x \in \mathbb{R}^d$ we think of $\mathbb{Z}^\theta(x) \in \mathbb{R}^d$ as an appropriate approximation

$$\mathbb{Z}^\theta(x) \approx (\nabla_x u)(0, x) \quad (70)$$

of $(\nabla_x u)(0, x) \in \mathbb{R}^d$, for all suitable $\theta \in \mathbb{R}^\nu$, $x \in \mathbb{R}^d$ and all $n \in \{0, 1, \dots, N-1\}$ we think of $\mathbb{G}_n^\theta(x) \in \mathbb{R}^{d \times d}$ as an appropriate approximation

$$\mathbb{G}_n^\theta(x) \approx (\text{Hess}_x u)(t_n, x) \quad (71)$$

of $(\text{Hess}_x u)(t_n, x) \in \mathbb{R}^{d \times d}$, and for all suitable $\theta \in \mathbb{R}^\nu$, $x \in \mathbb{R}^d$ and all $n \in \{0, 1, \dots, N-1\}$ we think of $\mathbb{A}_n^\theta(x) \in \mathbb{R}^d$ as an appropriate approximation

$$\mathbb{A}_n^\theta(x) \approx (\mathcal{L}(\nabla_x u))(t_n, x) \quad (72)$$

of $(\mathcal{L}(\nabla_x u))(t_n, x) \in \mathbb{R}^d$.

3.6 Stochastic gradient descent-type optimization

As in Subsection 2.6 we intend to reach a *suitable* $\theta \in \mathbb{R}^\nu$ in (67)–(72) by applying a minimization algorithm to the function

$$\mathbb{R}^\nu \ni \theta \mapsto \mathbb{E}[|\mathcal{Y}_N^\theta - g(\mathcal{X}_N)|^2] \in \mathbb{R}. \quad (73)$$

Applying a stochastic gradient descent-based minimization algorithm yields under suitable assumptions random approximations $\Theta_m: \Omega \rightarrow \mathbb{R}^\nu$, $m \in \mathbb{N}_0$, of a local minimum point of the function in (73). For sufficiently large $N, \nu, m \in \mathbb{N}$ we use under suitable hypotheses the random function

$$\mathbb{U}^{\Theta_m}: \Omega \rightarrow C(\mathbb{R}^d, \mathbb{R}) \quad (74)$$

as an appropriate approximation of the function

$$\mathbb{R}^d \ni x \mapsto u(0, x) \in \mathbb{R}. \quad (75)$$

A more detailed description is provided in the next subsection.

3.7 Framework for the algorithm in the general case

In this subsection we provide a general framework (see Framework 3.2 below) which covers the deep 2BSDE method derived in Subsections 3.1–3.6. The variant of the deep 2BSDE method described in Subsection 2.7 still remains the core idea of Framework 3.2. However, Framework 3.2 allows more general Itô processes as background dynamics (see (40), (49), (59), and (64) above and (76) below) than just Brownian motion (see Framework 2.1 in Subsection 2.7 above), Framework 3.2 allows to incorporate other minimization algorithms (cf. (82) below and, e.g., E, Han, & Jentzen [33, Subsections 3.2, 5.1, and 5.2]) such as the Adam optimizer (cf. Kingma & Ba [60] and (101)–(102) below) than just the plain vanilla stochastic gradient descent method (see, e.g., (35)–(36) in Framework 2.1 in Subsection 2.7 above), and Framework 3.2 allows to deploy more sophisticated machine learning techniques like batch normalization (cf. Ioffe & Szegedy [57] and (81) below). In Section 4 below we illustrate the general description in Framework 3.2 by several examples.

Framework 3.2 (General Case). Let $T \in (0, \infty)$, $N, d, \varrho, \varsigma, \nu \in \mathbb{N}$, let $f: [0, T] \times \mathbb{R}^d \times \mathbb{R} \times \mathbb{R}^d \times \mathbb{R}^{d \times d} \rightarrow \mathbb{R}$ and $g: \mathbb{R}^d \rightarrow \mathbb{R}$ be functions, let $(\Omega, \mathcal{F}, \mathbb{P}, (\mathbb{F}_t)_{t \in [0, T]})$ be a filtered probability space, let $W^{m,j}: [0, T] \times \Omega \rightarrow \mathbb{R}^d$, $m \in \mathbb{N}_0$, $j \in \mathbb{N}$, be independent standard $(\mathbb{F}_t)_{t \in [0, T]}$ -Brownian motions on $(\Omega, \mathcal{F}, \mathbb{P})$, let $\xi^{m,j}: \Omega \rightarrow \mathbb{R}^d$, $m \in \mathbb{N}_0$, $j \in \mathbb{N}$, be i.i.d. $\mathbb{F}_0/\mathcal{B}(\mathbb{R}^d)$ -measurable functions, let $t_0, t_1, \dots, t_N \in [0, T]$ be real numbers with $0 = t_0 < t_1 < \dots < t_N = T$, let $H: [0, T]^2 \times \mathbb{R}^d \times \mathbb{R}^d \rightarrow \mathbb{R}^d$ and $\sigma: \mathbb{R}^d \rightarrow \mathbb{R}^{d \times d}$ be functions, for every $\theta \in \mathbb{R}^\nu$ let $\mathbb{U}^\theta: \mathbb{R}^d \rightarrow \mathbb{R}$ and $\mathbb{Z}^\theta: \mathbb{R}^d \rightarrow \mathbb{R}^d$ be functions, for every $m \in \mathbb{N}_0$, $j \in \mathbb{N}$ let $\mathcal{X}^{m,j}: \{0, 1, \dots, N\} \times \Omega \rightarrow \mathbb{R}^d$ be a stochastic process which satisfies for all $n \in \{0, 1, \dots, N-1\}$ that $\mathcal{X}_0^{m,j} = \xi^{m,j}$ and

$$\mathcal{X}_{n+1}^{m,j} = H(t_n, t_{n+1}, \mathcal{X}_n^{m,j}, W_{t_{n+1}}^{m,j} - W_{t_n}^{m,j}), \quad (76)$$

for every $\theta \in \mathbb{R}^\nu$, $j \in \mathbb{N}$, $\mathbf{s} \in \mathbb{R}^\varsigma$, $n \in \{0, 1, \dots, N-1\}$ let $\mathbb{G}_n^{\theta,j,\mathbf{s}}: (\mathbb{R}^d)^{\mathbb{N}_0} \rightarrow \mathbb{R}^{d \times d}$ and $\mathbb{A}_n^{\theta,j,\mathbf{s}}: (\mathbb{R}^d)^{\mathbb{N}_0} \rightarrow \mathbb{R}^d$ be functions, for every $\theta \in \mathbb{R}^\nu$, $m \in \mathbb{N}_0$, $j \in \mathbb{N}$, $\mathbf{s} \in \mathbb{R}^\varsigma$ let $\mathcal{Y}^{\theta,m,j,\mathbf{s}}: \{0, 1, \dots, N\} \times \Omega \rightarrow \mathbb{R}$ and $\mathcal{Z}^{\theta,m,j,\mathbf{s}}: \{0, 1, \dots, N\} \times \Omega \rightarrow \mathbb{R}^d$ be stochastic processes which satisfy $\mathcal{Y}_0^{\theta,m,j,\mathbf{s}} = \mathbb{U}^\theta(\xi^{m,j})$ and $\mathcal{Z}_0^{\theta,m,j,\mathbf{s}} = \mathbb{Z}^\theta(\xi^{m,j})$ and which satisfy for all $n \in \{0, 1, \dots, N-1\}$ that

$$\begin{aligned} \mathcal{Y}_{n+1}^{\theta,m,j,\mathbf{s}} &= \mathcal{Y}_n^{\theta,m,j,\mathbf{s}} + (t_{n+1} - t_n) \left[\frac{1}{2} \text{Trace} \left(\sigma(\mathcal{X}_n^{m,j}) \sigma(\mathcal{X}_n^{m,j})^* \mathbb{G}_n^{\theta,j,\mathbf{s}}((\mathcal{X}_n^{m,i})_{i \in \mathbb{N}}) \right) \right. \\ &\quad \left. + f(t_n, \mathcal{X}_n^{m,j}, \mathcal{Y}_n^{\theta,m,j,\mathbf{s}}, \mathcal{Z}_n^{\theta,m,j,\mathbf{s}}, \mathbb{G}_n^{\theta,j,\mathbf{s}}((\mathcal{X}_n^{m,i})_{i \in \mathbb{N}})) \right] + \langle \mathcal{Z}_n^{\theta,m,j,\mathbf{s}}, \mathcal{X}_{n+1}^{m,j} - \mathcal{X}_n^{m,j} \rangle_{\mathbb{R}^d} \end{aligned} \quad (77)$$

and

$$\mathcal{Z}^{\theta,m,j,\mathbf{s}} = \mathbb{A}_n^{\theta,j,\mathbf{s}}((\mathcal{X}_n^{m,i})_{i \in \mathbb{N}}) (t_{n+1} - t_n) + \mathbb{G}_n^{\theta,j,\mathbf{s}}((\mathcal{X}_n^{m,i})_{i \in \mathbb{N}}) (\mathcal{X}_{n+1}^{m,j} - \mathcal{X}_n^{m,j}), \quad (78)$$

let $(J_m)_{m \in \mathbb{N}_0} \subseteq \mathbb{N}$ be a sequence, for every $m \in \mathbb{N}_0$, $\mathbf{s} \in \mathbb{R}^\varsigma$ let $\phi^{m,\mathbf{s}}: \mathbb{R}^\nu \times \Omega \rightarrow \mathbb{R}$ be the function which satisfies for all $(\theta, \omega) \in \mathbb{R}^\nu \times \Omega$ that

$$\phi^{m,\mathbf{s}}(\theta, \omega) = \frac{1}{J_m} \sum_{j=1}^{J_m} |\mathcal{Y}_N^{\theta,m,j,\mathbf{s}}(\omega) - g(\mathcal{X}_N^{m,j}(\omega))|^2, \quad (79)$$

for every $m \in \mathbb{N}_0$, $\mathbf{s} \in \mathbb{R}^\varsigma$ let $\Phi^{m,\mathbf{s}}: \mathbb{R}^\nu \times \Omega \rightarrow \mathbb{R}^\nu$ a function which satisfies for all $\omega \in \Omega$, $\theta \in \{\eta \in \mathbb{R}^\nu: \phi^{m,\mathbf{s}}(\cdot, \omega): \mathbb{R}^\nu \rightarrow \mathbb{R} \text{ is differentiable at } \eta\}$ that

$$\Phi^{m,\mathbf{s}}(\theta, \omega) = (\nabla_\theta \phi^{m,\mathbf{s}})(\theta, \omega), \quad (80)$$

let $\mathcal{S}: \mathbb{R}^\varsigma \times \mathbb{R}^\nu \times (\mathbb{R}^d)^{\{0,1,\dots,N-1\} \times \mathbb{N}} \rightarrow \mathbb{R}^\varsigma$ be a function, for every $m \in \mathbb{N}_0$ let $\psi_m: \mathbb{R}^\varrho \rightarrow \mathbb{R}^\nu$ and $\Psi_m: \mathbb{R}^\varrho \times \mathbb{R}^\nu \rightarrow \mathbb{R}^\varrho$ be functions, let $\Theta: \mathbb{N}_0 \times \Omega \rightarrow \mathbb{R}^\nu$, $\mathbb{S}: \mathbb{N}_0 \times \Omega \rightarrow \mathbb{R}^\varsigma$, and $\Xi: \mathbb{N}_0 \times \Omega \rightarrow \mathbb{R}^\varrho$ be stochastic processes which satisfy for all $m \in \mathbb{N}_0$ that

$$\mathbb{S}_{m+1} = \mathcal{S}(\mathbb{S}_m, \Theta_m, (\mathcal{X}_n^{m,i})_{(n,i) \in \{0,1,\dots,N-1\} \times \mathbb{N}}), \quad (81)$$

$$\Xi_{m+1} = \Psi_m(\Xi_m, \Phi^{m,\mathbb{S}_{m+1}}(\Theta_m)), \quad \text{and} \quad \Theta_{m+1} = \Theta_m - \psi_m(\Xi_{m+1}). \quad (82)$$

Under suitable further assumptions, we think in the case of sufficiently large $N, \nu \in \mathbb{N}$, $m \in \mathbb{N}_0$ in Framework 3.2 of the random variable $\Theta_m: \Omega \rightarrow \mathbb{R}^\nu$ as an appropriate approximation of a local minimum point of the expected loss function and we think in the case of sufficiently large $N, \nu \in \mathbb{N}$, $m \in \mathbb{N}_0$ in Framework 3.2 of the random function

$$\mathbb{R}^d \ni x \mapsto \mathbb{U}^{\Theta_m}(x, \omega) \in \mathbb{R}^d \quad (83)$$

for $\omega \in \Omega$ as an appropriate approximation of the function

$$\mathbb{R}^d \ni x \mapsto u(0, x) \in \mathbb{R} \quad (84)$$

where $u: [0, T] \times \mathbb{R}^d \rightarrow \mathbb{R}$ is an at most polynomially growing continuous function which satisfies for all $(t, x) \in [0, T] \times \mathbb{R}^d$ that $u|_{[0, T] \times \mathbb{R}^d} \in C^{1,2}([0, T] \times \mathbb{R}^d)$, $u(T, x) = g(x)$, and

$$\frac{\partial u}{\partial t}(t, x) = f(t, x, u(t, x), (\nabla_x u)(t, x), (\text{Hess}_x u)(t, x)) \quad (85)$$

(cf. (37) in Subsection 2.7). This terminal value problem can in a straight-forward manner be transformed into an initial value problem. This is the subject of the following elementary remark.

Remark 3.3. *Let $d \in \mathbb{N}$, $T \in (0, \infty)$, let $f: [0, T] \times \mathbb{R}^d \times \mathbb{R} \times \mathbb{R}^d \times \mathbb{R}^{d \times d} \rightarrow \mathbb{R}$ and $g: \mathbb{R}^d \rightarrow \mathbb{R}$ be functions, let $u: [0, T] \times \mathbb{R}^d \rightarrow \mathbb{R}$ be a continuous function which satisfies for all $(t, x) \in [0, T] \times \mathbb{R}^d$ that $u(T, x) = g(x)$, $u|_{[0, T] \times \mathbb{R}^d} \in C^{1,2}([0, T] \times \mathbb{R}^d, \mathbb{R})$, and*

$$\frac{\partial u}{\partial t}(t, x) = f(t, x, u(t, x), (\nabla_x u)(t, x), (\text{Hess}_x u)(t, x)), \quad (86)$$

and let $F: [0, T] \times \mathbb{R}^d \times \mathbb{R} \times \mathbb{R}^d \times \mathbb{R}^{d \times d} \rightarrow \mathbb{R}$ and $U: [0, T] \times \mathbb{R}^d \rightarrow \mathbb{R}$ be the functions which satisfy for all $(t, x, y, z, \gamma) \in [0, T] \times \mathbb{R}^d \times \mathbb{R} \times \mathbb{R}^d \times \mathbb{R}^{d \times d}$ that $U(t, x) = u(T - t, x)$ and

$$F(t, x, y, z, \gamma) = -f(T - t, x, y, z, \gamma). \quad (87)$$

Then it holds that $U: [0, T] \times \mathbb{R}^d \rightarrow \mathbb{R}$ is a continuous function which satisfies for all $(t, x) \in (0, T] \times \mathbb{R}^d$ that $U(0, x) = g(x)$, $U|_{(0, T] \times \mathbb{R}^d} \in C^{1,2}((0, T] \times \mathbb{R}^d, \mathbb{R})$, and

$$\frac{\partial U}{\partial t}(t, x) = F(t, x, U(t, x), (\nabla_x U)(t, x), (\text{Hess}_x U)(t, x)). \quad (88)$$

Proof of Remark 3.3. First, note that the hypothesis that $u: [0, T] \times \mathbb{R}^d \rightarrow \mathbb{R}$ is a continuous function ensures that $U: [0, T] \times \mathbb{R}^d \rightarrow \mathbb{R}$ is a continuous function. Next, note that for all $x \in \mathbb{R}^d$ it holds that

$$U(0, x) = u(T, x) = g(x). \quad (89)$$

Moreover, observe that the chain rule, (86), and (87) ensure that for all $(t, x) \in (0, T] \times \mathbb{R}^d$ it holds that $U|_{(0, T] \times \mathbb{R}^d} \in C^{1,2}((0, T] \times \mathbb{R}^d, \mathbb{R})$, $U(0, x) = g(x)$, and

$$\begin{aligned} \frac{\partial U}{\partial t}(t, x) &= \frac{\partial}{\partial t} [u(T - t, x)] = -\left(\frac{\partial u}{\partial t}\right)(T - t, x) \\ &= -f(T - t, x, u(T - t, x), (\nabla_x u)(T - t, x), (\text{Hess}_x u)(T - t, x)) \\ &= -f(T - t, x, U(t, x), (\nabla_x U)(t, x), (\text{Hess}_x U)(t, x)) \\ &= F(t, x, U(t, x), (\nabla_x U)(t, x), (\text{Hess}_x U)(t, x)). \end{aligned} \quad (90)$$

Combining the fact that $U: [0, T] \times \mathbb{R}^d \rightarrow \mathbb{R}$ is a continuous function with (89) and (90) completes the proof of Remark 3.3. \square

4 Examples

In this section we employ the deep 2BSDE method (see Framework 2.1 and Framework 3.2 above) to approximate the solutions of several example PDEs such as Allen-Cahn equations, a Hamilton-Jacobi-Bellman (HJB) equation, a Black-Scholes-Barenblatt equation, and nonlinear expectations of G -Brownian motions. More specifically, in Subsection 4.1 we employ an implementation of the deep 2BSDE method in Framework 2.1 to approximate a 20-dimensional Allen-Cahn equation, in Subsection 4.3 we employ an implementation of the deep 2BSDE method in Framework 3.2 to approximate a 100-dimensional Black-Scholes-Barenblatt equation, in Subsection 4.4 we employ an implementation of the deep 2BSDE method in Framework 3.2 to approximate a 100-dimensional Hamilton-Jacobi-Bellman equation, in Subsection 4.5 we employ an implementation of the deep 2BSDE method in Framework 3.2 to approximate a 50-dimensional Allen-Cahn equation, and in Subsection 4.6 we employ implementations of the deep 2BSDE method in Framework 3.2 to approximate nonlinear expectations of G -Brownian motions in 1 and 100 space-dimensions. The PYTHON code used for the implementation of the deep 2BSDE method in Subsection 4.1 can be found in Subsection A.1 below. The PYTHON code used for the implementation of the deep 2BSDE method in Subsection 4.3 can be found in Subsection A.3 below. All of the numerical experiments presented below have been performed in PYTHON 3.6 using TENSORFLOW 1.2 or TENSORFLOW 1.3, respectively, on a LENOVO X1 CARBON with a 2.40 Gigahertz (GHz) INTEL i7 microprocessor with 8 Megabytes (MB) RAM.

4.1 Allen-Cahn equation with plain gradient descent and no batch normalization

In this subsection we use the deep 2BSDE method in Framework 2.1 to approximatively calculate the solution of a 20-dimensional Allen-Cahn equation with a cubic nonlinearity (see (98) below).

Assume Framework 2.1, assume that $T = \frac{3}{10}$, $\gamma = \frac{1}{1000}$, $d = 20$, $N = 20$, $\xi = 0 \in \mathbb{R}^{20}$, $\nu \geq (5Nd + Nd^2 + 1)(d + 1)$, assume for every $\theta = (\theta_1, \dots, \theta_\nu) \in \mathbb{R}^\nu$, $x \in \mathbb{R}^d$ that

$$\mathbb{G}_0^\theta(x) = \begin{pmatrix} \theta_{d+2} & \theta_{d+3} & \dots & \theta_{2d+1} \\ \theta_{2d+2} & \theta_{2d+3} & \dots & \theta_{3d+1} \\ \vdots & \vdots & \vdots & \vdots \\ \theta_{d^2+2} & \theta_{d^3+3} & \dots & \theta_{d^2+d+1} \end{pmatrix} \in \mathbb{R}^{d \times d} \quad \text{and} \quad \mathbb{A}_0^\theta(x) = \begin{pmatrix} \theta_{d^2+d+2} \\ \theta_{d^2+d+3} \\ \vdots \\ \theta_{d^2+2d+1} \end{pmatrix} \in \mathbb{R}^d, \quad (91)$$

for every $k \in \mathbb{N}$ let $\mathcal{R}_k: \mathbb{R}^k \rightarrow \mathbb{R}^k$ be the function which satisfies for all $x = (x_1, \dots, x_k) \in$

\mathbb{R}^k that

$$\mathcal{R}_k(x) = (\max\{x_1, 0\}, \dots, \max\{x_k, 0\}), \quad (92)$$

for every $\theta = (\theta_1, \dots, \theta_\nu) \in \mathbb{R}^\nu$, $v \in \mathbb{N}_0$, $k, l \in \mathbb{N}$ with $v + k(l + 1) \leq \nu$ let $M_{k,l}^{\theta,v} : \mathbb{R}^l \rightarrow \mathbb{R}^k$ be the affine linear function which satisfies for all $x = (x_1, \dots, x_l)$ that

$$M_{k,l}^{\theta,v}(x) = \begin{pmatrix} \theta_{v+1} & \theta_{v+2} & \dots & \theta_{v+l} \\ \theta_{v+l+1} & \theta_{v+l+2} & \dots & \theta_{v+2l} \\ \theta_{v+2l+1} & \theta_{v+2l+2} & \dots & \theta_{v+3l} \\ \vdots & \vdots & \vdots & \vdots \\ \theta_{v+(k-1)l+1} & \theta_{v+(k-1)l+2} & \dots & \theta_{v+kl} \end{pmatrix} \begin{pmatrix} x_1 \\ x_2 \\ x_3 \\ \vdots \\ x_l \end{pmatrix} + \begin{pmatrix} \theta_{v+kl+1} \\ \theta_{v+kl+2} \\ \theta_{v+kl+3} \\ \vdots \\ \theta_{v+kl+k} \end{pmatrix}, \quad (93)$$

assume for all $\theta \in \mathbb{R}^\nu$, $n \in \{1, 2, \dots, N-1\}$, $x \in \mathbb{R}^d$ that

$$\mathbb{A}_n^\theta = M_{d,d}^{\theta,[(2N+n)d+1](d+1)} \circ \mathcal{R}_d \circ M_{d,d}^{\theta,[(N+n)d+1](d+1)} \circ \mathcal{R}_d \circ M_{d,d}^{\theta,(nd+1)(d+1)} \quad (94)$$

and

$$\mathbb{G}_n^\theta = M_{d^2,d}^{\theta,(5Nd+nd^2+1)(d+1)} \circ \mathcal{R}_d \circ M_{d,d}^{\theta,[(4N+n)d+1](d+1)} \circ \mathcal{R}_d \circ M_{d,d}^{\theta,[(3N+n)d+1](d+1)}, \quad (95)$$

assume for all $i \in \{0, 1, \dots, N\}$, $\theta \in \mathbb{R}^\nu$, $t \in [0, T]$, $x, z \in \mathbb{R}^d$, $y \in \mathbb{R}$, $S \in \mathbb{R}^{d \times d}$ that $t_i = \frac{iT}{N}$, $g(x) = [2 + \frac{2}{5}\|x\|_{\mathbb{R}^d}^2]^{-1}$, and

$$f(t, x, y, z, S) = -\frac{1}{2} \text{Trace}(S) - y + y^3, \quad (96)$$

and let $u : [0, T] \times \mathbb{R}^d \rightarrow \mathbb{R}$ be an at most polynomially growing continuous function which satisfies for all $(t, x) \in [0, T] \times \mathbb{R}^d$ that $u(T, x) = g(x)$, $u|_{[0,T] \times \mathbb{R}^d} \in C^{1,2}([0, T] \times \mathbb{R}^d, \mathbb{R})$, and

$$\frac{\partial u}{\partial t}(t, x) = f(t, x, u(t, x), (\nabla_x u)(t, x), (\text{Hess}_x u)(t, x)). \quad (97)$$

The solution $u : [0, T] \times \mathbb{R}^d \rightarrow \mathbb{R}$ of the PDE (97) satisfies for all $(t, x) \in [0, T] \times \mathbb{R}^d$ that $u(T, x) = [2 + \frac{2}{5}\|x\|_{\mathbb{R}^d}^2]^{-1}$ and

$$\frac{\partial u}{\partial t}(t, x) + \frac{1}{2}(\Delta_x u)(t, x) + u(t, x) - [u(t, x)]^3 = 0. \quad (98)$$

In Table 1 we use PYTHON code 1 in Subsection A.1 below to approximatively calculate the mean of $\Theta_m^{(1)}$, the standard deviation of $\Theta_m^{(1)}$, the relative L^1 -approximation error associated to $\Theta_m^{(1)}$, the uncorrected sample standard deviation of the relative approximation error associated to $\Theta_m^{(1)}$, the mean of the loss function associated to Θ_m , the standard deviation of the loss function associated to Θ_m , and the average runtime in seconds needed for calculating one realization of $\Theta_m^{(1)}$ against $m \in \{0, 1000, 2000, 3000, 4000, 5000\}$ based on 10 independent realizations (10 independent runs of PYTHON code 1 in Subsection A.1 below). In addition, Figure 1 depicts approximations of the relative L^1 -approximation

Number of iteration steps	Mean of \mathcal{U}^{Θ_m}	Standard deviation of \mathcal{U}^{Θ_m}	Rel. L^1 -approx. error	Standard deviation of the relative approx. error	Mean of the loss function	Standard deviation of the loss function	Runtime in sec. for one realiz. of \mathcal{U}^{Θ_m}
0	-0.02572	0.6954	2.1671	1.24464	0.50286	0.58903	3
1000	0.19913	0.1673	0.5506	0.34117	0.02313	0.01927	6
2000	0.27080	0.0504	0.1662	0.11875	0.00758	0.00672	8
3000	0.29543	0.0129	0.0473	0.03709	0.01014	0.01375	11
4000	0.30484	0.0054	0.0167	0.01357	0.01663	0.02106	13
5000	0.30736	0.0030	0.0093	0.00556	0.00575	0.00985	15

Table 1: Numerical simulations of the deep2BSDE method in Framework 2.1 in the case of the 20-dimensional Allen-Cahn equation (98) (cf. PYTHON code 1 in Subsection A.1 below). In the approximative calculations of the relative L^1 -approximation errors the value $u(0, \xi)$ has been replaced by the value 0.30879 which has been calculated through the Branching diffusion method (cf. MATLAB code 2 in Subsection A.2 below).

error and approximations of the mean of the loss function associated to $\Theta_m^{(1)}$ against $m \in \{0, 1, 2, \dots, 5000\}$ based on 10 independent realizations (10 independent runs of PYTHON code 1 in Subsection A.1 below). In the approximative calculations of the relative L^1 -approximation errors in Table 1 and Figure 1 the value $u(0, \xi)$ of the solution u of the PDE (98) has been replaced by the value 0.30879 which, in turn, has been calculated through the Branching diffusion method (see MATLAB code 2 in Appendix A.2 below).

4.2 Setting for the deep 2BSDE method with batch normalization and the Adam optimizer

Assume Framework 3.2, let $\varepsilon \in (0, \infty)$, $\beta_1 = \frac{9}{10}$, $\beta_2 = \frac{999}{1000}$, $(\gamma_m)_{m \in \mathbb{N}_0} \subseteq (0, \infty)$, let $\text{Pow}_r: \mathbb{R}^\nu \rightarrow \mathbb{R}^\nu$, $r \in (0, \infty)$, be the functions which satisfy for all $r \in (0, \infty)$, $x = (x_1, \dots, x_\nu) \in \mathbb{R}^\nu$ that

$$\text{Pow}_r(x) = (|x_1|^r, \dots, |x_\nu|^r), \quad (99)$$

let $u: [0, T] \times \mathbb{R}^d \rightarrow \mathbb{R}$ be an at most polynomially growing continuous function which satisfies for all $(t, x) \in [0, T) \times \mathbb{R}^d$ that $u(T, x) = g(x)$, $u|_{[0, T) \times \mathbb{R}^d} \in C^{1,2}([0, T) \times \mathbb{R}^d, \mathbb{R})$, and

$$\frac{\partial u}{\partial t}(t, x) = f(t, x, u(t, x), (\nabla_x u)(t, x), (\text{Hess}_x u)(t, x)), \quad (100)$$

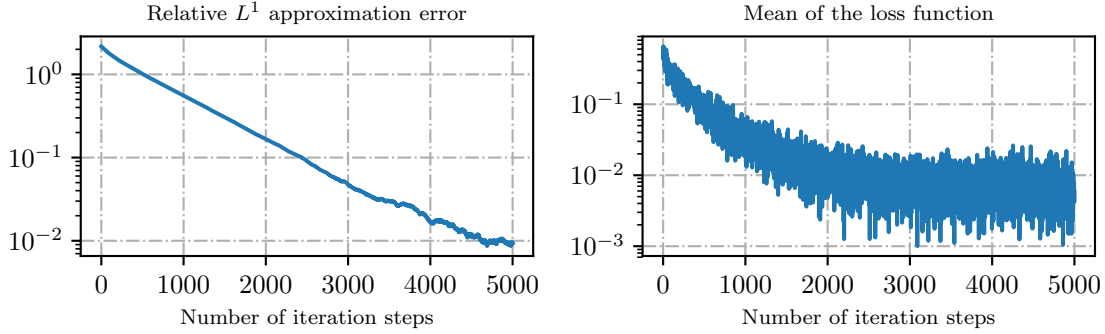


Figure 1: Plots of approximative calculations of the relative L^1 -approximation error $\mathbb{E}\left[\frac{|\Theta_m^{(1)} - 0.30879|}{0.30879}\right]$ and of the mean of the loss function $\mathbb{E}[|\mathcal{Y}_N^{m, \Theta_m} - g(\xi + W_T^m)|^2]$ in the case of the 20-dimensional Allen-Cahn equation (98) against $m \in \{0, 1, \dots, 5000\}$.

assume for all $m \in \mathbb{N}_0$, $i \in \{0, 1, \dots, N\}$ that $J_m = 64$, $t_i = \frac{iT}{N}$, and $\varrho = 2\nu$, and assume for all $m \in \mathbb{N}_0$, $x = (x_1, \dots, x_\nu)$, $y = (y_1, \dots, y_\nu) \in \mathbb{R}^\nu$, $\eta = (\eta_1, \dots, \eta_\nu) \in \mathbb{R}^\nu$ that

$$\Psi_m(x, y, \eta) = (\beta_1 x + (1 - \beta_1)\eta, \beta_2 y + (1 - \beta_2)\text{Pow}_2(\eta)) \quad (101)$$

and

$$\psi_m(x, y) = \left(\left[\sqrt{\frac{|y_1|}{1 - \beta_2^m}} + \varepsilon \right]^{-1} \frac{\gamma_m x_1}{1 - \beta_1^m}, \dots, \left[\sqrt{\frac{|y_\nu|}{1 - \beta_2^m}} + \varepsilon \right]^{-1} \frac{\gamma_m x_\nu}{1 - \beta_1^m} \right). \quad (102)$$

Remark 4.1. Equations (101) and (102) describe the Adam optimizer; cf. Kingma & Ba [60] and lines 181–186 in PYTHON code 3 in Subsection A.3 below. The default choice in TENSORFLOW for the real number $\varepsilon \in (0, \infty)$ in (102) is $\varepsilon = 10^{-8}$ but according to the comments in the file `adam.py` in TENSORFLOW there are situations in which other choices may be more appropriate. In Subsection 4.5 we took $\varepsilon = 1$ (in which case one has to add the argument `epsilon=1.0` to `tf.train.AdamOptimizer` in lines 181–183 in PYTHON code 3 in Subsection A.3 below) whereas we used the default value $\varepsilon = 10^{-8}$ in Subsections 4.3, 4.4, and 4.6.

4.3 A 100-dimensional Black-Scholes-Barenblatt equation

In this subsection we use the deep 2BSDE method in Framework 3.2 to approximatively calculate the solution of a 100-dimensional Black-Scholes-Barenblatt equation (see Avellaneda, Levy, & Parás [2] and (105) below).

Assume the setting of Subsection 4.2, assume $d = 100$, $T = 1$, $N = 20$, $\varepsilon = 10^{-8}$, assume for all $\omega \in \Omega$ that $\xi(\omega) = (1, 1/2, 1, 1/2, \dots, 1, 1/2) \in \mathbb{R}^d$, let $r = \frac{5}{100}$, $\sigma_{\max} = \frac{4}{10}$,

Number of iteration steps	Mean of \mathcal{U}^{Θ_m}	Standard deviation of \mathcal{U}^{Θ_m}	Rel. L^1 -approx. error	Standard deviation of the relative approx. error	Mean of the empirical loss function	Standard deviation of the empirical loss function	Runtime in sec. for one realiz. of \mathcal{U}^{Θ_m}
0	0.522	0.2292	0.9932	0.00297	5331.35	101.28	25
100	56.865	0.5843	0.2625	0.00758	441.04	90.92	191
200	74.921	0.2735	0.0283	0.00355	173.91	40.28	358
300	76.598	0.1636	0.0066	0.00212	96.56	17.61	526
400	77.156	0.1494	0.0014	0.00149	66.73	18.27	694

Table 2: Numerical simulations of the deep2BSDE method in Framework 3.2 in the case of the 100-dimensional Black-Scholes-Barenblatt equation (105) (cf. PYTHON code 3 in Subsection A.3 below). In the approximative calculations of the relative L^1 -approximation errors the value $u(0, (1, 1/2, 1, 1/2, \dots, 1, 1/2))$ has been replaced by the value 77.1049 which has been calculated by means of Lemma 4.2.

$\sigma_{\min} = \frac{1}{10}$, $\sigma_c = \frac{4}{10}$, let $\bar{\sigma}: \mathbb{R} \rightarrow \mathbb{R}$ be the function which satisfies for all $x \in \mathbb{R}$ that

$$\bar{\sigma}(x) = \begin{cases} \sigma_{\max} & : x \geq 0 \\ \sigma_{\min} & : x < 0 \end{cases}, \quad (103)$$

assume for all $s, t \in [0, T]$, $x = (x_1, \dots, x_d)$, $w = (w_1, \dots, w_d)$, $z = (z_1, \dots, z_d) \in \mathbb{R}^d$, $y \in \mathbb{R}$, $S = (S_{ij})_{(i,j) \in \{1, \dots, d\}^2} \in \mathbb{R}^{d \times d}$ that $\sigma(x) = \sigma_c \text{diag}(x_1, \dots, x_d)$, $H(s, t, x, w) = x + \sigma(x)w$, $g(x) = \|x\|_{\mathbb{R}^d}^2$, and

$$f(t, x, y, z, S) = -\frac{1}{2} \sum_{i=1}^d |x_i|^2 |\bar{\sigma}(S_{ii})|^2 S_{ii} + r(y - \langle x, z \rangle_{\mathbb{R}^d}). \quad (104)$$

The solution $u: [0, T] \times \mathbb{R}^d \rightarrow \mathbb{R}$ of the PDE (100) then satisfies for all $(t, x) \in [0, T] \times \mathbb{R}^d$ that $u(T, x) = \|x\|_{\mathbb{R}^d}^2$ and

$$\frac{\partial u}{\partial t}(t, x) + \frac{1}{2} \sum_{i=1}^d |x_i|^2 |\bar{\sigma}(\frac{\partial^2 u}{\partial x_i^2}(t, x))|^2 \frac{\partial^2 u}{\partial x_i^2}(t, x) = r(u(t, x) - \langle x, (\nabla_x u)(t, x) \rangle_{\mathbb{R}^d}). \quad (105)$$

In Table 2 we use PYTHON code 3 in Subsection A.3 below to approximatively calculate the mean $\mathbb{U}^{\Theta_m}(\xi)$, the standard deviation of $\mathbb{U}^{\Theta_m}(\xi)$, the relative L^1 -approximation error associated to $\mathbb{U}^{\Theta_m}(\xi)$, the uncorrected sample standard deviation of the relative approximation error associated to $\mathbb{U}^{\Theta_m}(\xi)$, the mean of the empirical loss function associated to Θ_m , the standard deviation of the empirical loss function associated to Θ_m , and

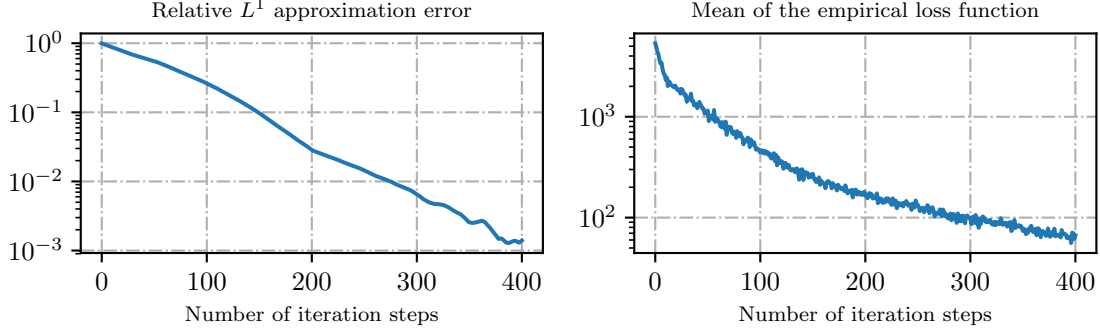


Figure 2: Plots of approximative calculations of the relative L^1 -approximation error $\mathbb{E} \left[\frac{|\mathbb{U}^{\Theta_m}(\xi) - 77.1049|}{77.1049} \right]$ and of the mean of the empirical loss function $\mathbb{E} \left[\frac{1}{J_m} \sum_{j=1}^{J_m} |\mathcal{Y}_N^{m, \Theta_m, j, \mathbb{S}_{m+1}} - g(\mathcal{X}_N^{m, j})|^2 \right]$ in the case of the 100-dimensional Black-Scholes-Barenblatt equation (105) against $m \in \{0, 1, \dots, 400\}$.

the average runtime in seconds needed for calculating one realization of $\mathbb{U}^{\Theta_m}(\xi)$ against $m \in \{0, 100, 200, 300, 400\}$ based on 10 realizations (10 independent runs of PYTHON code 3 in Subsection A.3 below). In addition, Figure 2 depicts approximations of the relative L^1 -approximation error and approximations of the mean of the empirical loss function associated to Θ_m against $m \in \{0, 1, \dots, 400\}$ based on 10 independent realizations (10 independent runs of PYTHON code 3). In the approximative calculations of the relative L^1 -approximation errors in Table 2 and Figure 2 the value $u(0, (1, 1/2, 1, 1/2, \dots, 1, 1/2))$ of the solution u of the PDE (105) has been replaced by the value 77.1049 which, in turn, has been calculated by means of Lemma 4.2 below.

Lemma 4.2. *Let $c, \sigma_{\max}, r, T \in (0, \infty)$, $\sigma_{\min} \in (0, \sigma_{\max})$, $d \in \mathbb{N}$, let $\bar{\sigma}: \mathbb{R} \rightarrow \mathbb{R}$ be the function which satisfies for all $x \in \mathbb{R}$ that*

$$\bar{\sigma}(x) = \begin{cases} \sigma_{\max} & : x \geq 0 \\ \sigma_{\min} & : x < 0 \end{cases}, \quad (106)$$

and let $g: \mathbb{R}^d \rightarrow \mathbb{R}$ and $u: [0, T] \times \mathbb{R}^d \rightarrow \mathbb{R}$ be the functions which satisfy for all $t \in [0, T]$, $x = (x_1, \dots, x_d) \in \mathbb{R}^d$ that $g(x) = c \|x\|_{\mathbb{R}^d}^2 = c \sum_{i=1}^d |x_i|^2$ and

$$u(t, x) = \exp([r + |\sigma_{\max}|^2](T - t)) g(x). \quad (107)$$

Then it holds for all $t \in [0, T]$, $x = (x_1, \dots, x_d) \in \mathbb{R}^d$ that $u \in C^\infty([0, T] \times \mathbb{R}^d, \mathbb{R})$, $u(T, x) = g(x)$, and

$$\frac{\partial u}{\partial t}(t, x) + \frac{1}{2} \sum_{i=1}^d |x_i|^2 |\bar{\sigma}(\frac{\partial^2 u}{\partial x_i^2}(t, x))|^2 \frac{\partial^2 u}{\partial x_i^2}(t, x) = r(u(t, x) - \langle x, (\nabla_x u)(t, x) \rangle_{\mathbb{R}^d}). \quad (108)$$

Proof of Lemma 4.2. Observe that the function u is clearly infinitely often differentiable. Next note that (107) ensures that for all $t \in [0, T]$, $x = (x_1, \dots, x_d) \in \mathbb{R}^d$ it holds that

$$u(t, x) = \exp(-t[r + |\sigma_{\max}|^2] + T[r + |\sigma_{\max}|^2]) g(x). \quad (109)$$

Hence, we obtain that for all $t \in [0, T]$, $x = (x_1, \dots, x_d) \in \mathbb{R}^d$, $i \in \{1, 2, \dots, d\}$ it holds that

$$\frac{\partial u}{\partial t}(t, x) = -[r + |\sigma_{\max}|^2]u(t, x), \quad (110)$$

$$\begin{aligned} \langle x, (\nabla_x u)(t, x) \rangle_{\mathbb{R}^d} &= \exp(-t[r + |\sigma_{\max}|^2] + T[r + |\sigma_{\max}|^2]) \langle x, (\nabla g)(x) \rangle_{\mathbb{R}^d} \\ &= \exp(-t[r + |\sigma_{\max}|^2] + T[r + |\sigma_{\max}|^2]) \langle x, 2cx \rangle_{\mathbb{R}^d} \\ &= 2c \exp(-t[r + |\sigma_{\max}|^2] + T[r + |\sigma_{\max}|^2]) \|x\|_{\mathbb{R}^d}^2 = 2u(t, x), \end{aligned} \quad (111)$$

and

$$\frac{\partial^2 u}{\partial x_i^2}(t, x) = 2c \exp(-t[r + |\sigma_{\max}|^2] + T[r + |\sigma_{\max}|^2]) > 0. \quad (112)$$

Combining this with (106) demonstrates that for all $t \in [0, T]$, $x = (x_1, \dots, x_d) \in \mathbb{R}^d$, $i \in \{1, 2, \dots, d\}$ it holds that

$$\bar{\sigma} \left(\frac{\partial^2 u}{\partial x_i^2}(t, x) \right) = \sigma_{\max}. \quad (113)$$

This and (110)–(112) ensure that for all $t \in [0, T]$, $x = (x_1, \dots, x_d) \in \mathbb{R}^d$ it holds that

$$\begin{aligned} &\frac{\partial u}{\partial t}(t, x) + \frac{1}{2} \sum_{i=1}^d |x_i|^2 \left| \bar{\sigma} \left(\frac{\partial^2 u}{\partial x_i^2}(t, x) \right) \right|^2 \frac{\partial^2 u}{\partial x_i^2}(t, x) - r(u(t, x) - \langle x, (\nabla_x u)(t, x) \rangle_{\mathbb{R}^d}) \\ &= -[r + |\sigma_{\max}|^2] u(t, x) + \frac{1}{2} \sum_{i=1}^d |x_i|^2 \left| \bar{\sigma} \left(\frac{\partial^2 u}{\partial x_i^2}(t, x) \right) \right|^2 \frac{\partial^2 u}{\partial x_i^2}(t, x) - r(u(t, x) - 2u(t, x)) \\ &= -[r + |\sigma_{\max}|^2] u(t, x) + \frac{1}{2} \sum_{i=1}^d |x_i|^2 |\sigma_{\max}|^2 \frac{\partial^2 u}{\partial x_i^2}(t, x) + ru(t, x) \\ &= \frac{1}{2} \sum_{i=1}^d |x_i|^2 |\sigma_{\max}|^2 \frac{\partial^2 u}{\partial x_i^2}(t, x) - |\sigma_{\max}|^2 u(t, x) = |\sigma_{\max}|^2 \left[\frac{1}{2} \sum_{i=1}^d |x_i|^2 \frac{\partial^2 u}{\partial x_i^2}(t, x) - u(t, x) \right] \\ &= |\sigma_{\max}|^2 \left[\frac{1}{2} \|x\|_{\mathbb{R}^d}^2 \frac{\partial^2 u}{\partial x_1^2}(t, x) - u(t, x) \right] \\ &= |\sigma_{\max}|^2 [c \|x\|_{\mathbb{R}^d}^2 \exp(-t[r + |\sigma_{\max}|^2] + T[r + |\sigma_{\max}|^2]) - u(t, x)] = 0. \end{aligned} \quad (114)$$

The proof of Lemma 4.2 is thus completed. \square

4.4 A 100-dimensional Hamilton-Jacobi-Bellman equation

In this subsection we use the deep 2BSDE method in Framework 3.2 to approximately calculate the solution of a 100-dimensional Hamilton-Jacobi-Bellman equation with a nonlinearity that is quadratic in the gradient (see, e.g., [33, Section 4.3] and (116) below).

Assume the setting of Subsection 4.2, assume $d = 100$, $T = 1$, $N = 20$, $\varepsilon = 10^{-8}$, assume for all $\omega \in \Omega$ that $\xi(\omega) = (0, 0, \dots, 0) \in \mathbb{R}^d$, and assume for all $m \in \mathbb{N}_0$, $s, t \in [0, T]$, $x, w, z \in \mathbb{R}^d$, $y \in \mathbb{R}$, $S \in \mathbb{R}^{d \times d}$ that $\sigma(x) = \sqrt{2} \text{Id}_{\mathbb{R}^d}$, $H(s, t, x, w) = x + \sqrt{2}w$, $\gamma_m = \frac{1}{100}$, $g(x) = \ln(\frac{1}{2}[1 + \|x\|_{\mathbb{R}^d}^2])$, and

$$f(t, x, y, z, S) = -\text{Trace}(S) + \|z\|_{\mathbb{R}^d}^2. \quad (115)$$

The solution $u: [0, T] \times \mathbb{R}^d \rightarrow \mathbb{R}$ of the PDE (100) then satisfies for all $(t, x) \in [0, T] \times \mathbb{R}^d$ that

$$\frac{\partial u}{\partial t}(t, x) + (\Delta_x u)(t, x) = \|\nabla_x u(t, x)\|_{\mathbb{R}^d}^2. \quad (116)$$

In Table 3 we use an adapted version of PYTHON code 3 in Subsection A.3 below to approximately calculate the mean of $\mathbb{U}^{\Theta_m}(\xi)$, the standard deviation of $\mathbb{U}^{\Theta_m}(\xi)$, the relative L^1 -approximation error associated to $\mathbb{U}^{\Theta_m}(\xi)$, the uncorrected sample standard deviation of the relative approximation error associated to $\mathbb{U}^{\Theta_m}(\xi)$, the mean of the empirical loss function associated to $\mathbb{U}^{\Theta_m}(\xi)$, the standard deviation of the empirical loss function associated to $\mathbb{U}^{\Theta_m}(\xi)$, and the average runtime in seconds needed for calculating one realization of $\mathbb{U}^{\Theta_m}(\xi)$ against $m \in \{0, 500, 1000, 1500, 2000\}$ based on 10 independent realizations (10 independent runs). In addition, Figure 3 depicts approximations of the mean of the relative L^1 -approximation error and approximations of the mean of the empirical loss function associated to Θ_m against $m \in \{0, 1, \dots, 2000\}$ based on 10 independent realizations (10 independent runs). In the calculation of the relative L^1 -approximation errors in Table 3 and Figure 3 the value $u(0, (0, 0, \dots, 0))$ of the solution of the PDE (116) has been replaced by the value 4.5901 which, in turn, was calculated by means of Lemma 4.2 in [33] (with $d = 100$, $T = 1$, $\alpha = 1$, $\beta = -1$, $g = \mathbb{R}^d \ni x \mapsto \ln(\frac{1}{2}[1 + \|x\|_{\mathbb{R}^d}^2]) \in \mathbb{R}$ in the notation of Lemma 4.2 in [33]) and the classical Monte Carlo method (cf. MATLAB code 4 in Appendix A.4 below).

4.5 A 50-dimensional Allen-Cahn equation

In this subsection we use the deep 2BSDE method in Framework 3.2 to approximately calculate the solution of a 50-dimensional Allen-Cahn equation with a cubic nonlinearity (see (118) below).

Assume the setting of Subsection 4.2, assume $T = \frac{3}{10}$, $N = 20$, $d = 50$, $\varepsilon = 1$, assume for all $\omega \in \Omega$ that $\xi(\omega) = (0, 0, \dots, 0) \in \mathbb{R}^{50}$, and assume for all $m \in \mathbb{N}_0$, $s, t \in [0, T]$, $x, w, z \in \mathbb{R}^d$, $y \in \mathbb{R}$, $S \in \mathbb{R}^{d \times d}$ that $\sigma(x) = \sqrt{2} \text{Id}_{\mathbb{R}^d}$, $H(s, t, x, w) = x + \sigma(x)w = x + \sqrt{2}w$, $g(x) = [2 + \frac{2}{5}\|x\|_{\mathbb{R}^d}^2]^{-1}$, $f(t, x, y, z, S) = -\text{Trace}(S) - y + y^3$, and

$$\gamma_m = \frac{1}{10} \cdot \left[\frac{9}{10} \right]^{\lfloor \frac{m}{1000} \rfloor}. \quad (117)$$

Number of iteration steps	Mean of \mathcal{U}^{Θ_m}	Standard deviation of \mathcal{U}^{Θ_m}	Rel. L^1 -approx. error	Standard deviation of the relative approx. error	Mean of the empirical loss function	Standard deviation of the empirical loss function	Runtime in sec. for one realiz. of \mathcal{U}^{Θ_m}
0	0.6438	0.2506	0.8597	0.05459	8.08967	1.65498	24
500	2.2008	0.1721	0.5205	0.03750	4.44386	0.51459	939
1000	3.6738	0.1119	0.1996	0.02437	1.46137	0.46636	1857
1500	4.4094	0.0395	0.0394	0.00860	0.26111	0.08805	2775
2000	4.5738	0.0073	0.0036	0.00159	0.05641	0.01412	3694

Table 3: Numerical simulations of the deep2BSDE method in Framework 3.2 in the case of the 100-dimensional Hamilton-Jacobi-Bellman equation (116). In the approximative calculations of the relative L^1 -approximation errors the value $u(0, (0, 0, \dots, 0))$ has been replaced by the value 4.5901 which has been calculated by means of the classical Monte Carlo method (cf. MATLAB code 4 in Appendix A.4 below).

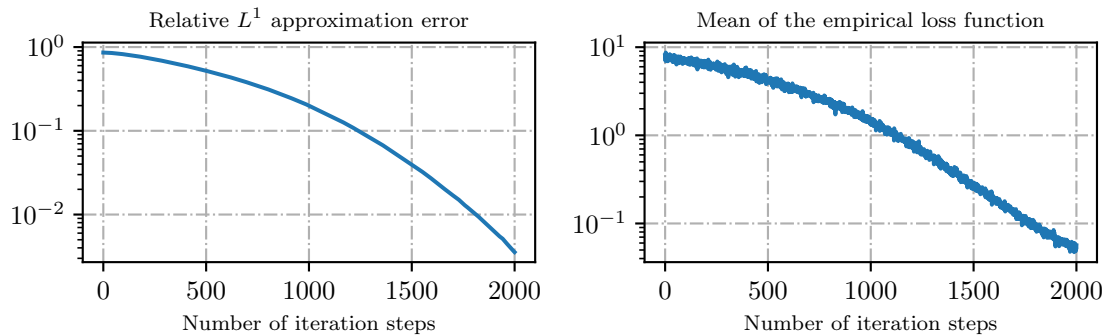


Figure 3: Plots of approximative calculations of the relative L^1 -approximation error $\mathbb{E}\left[\frac{|\mathcal{U}^{\Theta_m}(\xi) - 4.5901|}{4.5901}\right]$ and of the mean of the empirical loss function $\mathbb{E}\left[\frac{1}{J_m} \sum_{j=1}^{J_m} |\mathcal{Y}_N^{m, \Theta_m, j, S_{m+1}} - g(\mathcal{X}_N^{m, j})|^2\right]$ in the case of the 100-dimensional Hamilton-Jacobi-Bellman equation (116) against $m \in \{0, 1, \dots, 2000\}$.

Number of iteration steps	Mean of \mathcal{U}^{Θ_m}	Standard deviation of \mathcal{U}^{Θ_m}	Rel. L^1 -approx. error	Standard deviation of the relative approx. error	Mean of the empirical loss function	Standard deviation of the empirical loss function	Runtime in sec. for one realiz. of \mathcal{U}^{Θ_m}
0	0.5198	0.19361	4.24561	1.95385	0.5830	0.4265	22
500	0.0943	0.00607	0.06257	0.04703	0.0354	0.0072	212
1000	0.0977	0.00174	0.01834	0.01299	0.0052	0.0010	404
1500	0.0988	0.00079	0.00617	0.00590	0.0008	0.0001	595
2000	0.0991	0.00046	0.00371	0.00274	0.0003	0.0001	787

Table 4: Numerical simulations of the deep2BSDE method in Framework 3.2 in the case of the 50-dimensional Allen-Cahn equation (118). In the approximative calculations of the relative L^1 -approximation errors the value $u(0, (0, 0, \dots, 0))$ has been replaced by the value 0.09909 which has been calculated through the Branching diffusion method (cf. MATLAB code 2 in Subsection A.2 below).

The solution u to the PDE (100) then satisfies for all $(t, x) \in [0, T) \times \mathbb{R}^d$ that $u(T, x) = g(x)$ and

$$\frac{\partial u}{\partial t}(t, x) + \Delta u(t, x) + u(t, x) - [u(t, x)]^3 = 0. \quad (118)$$

In Table 4 we use an adapted version of PYTHON code 3 in Subsection A.3 below to approximatively calculate the mean $\mathbb{U}^{\Theta_m}(\xi)$, the standard deviation of $\mathbb{U}^{\Theta_m}(\xi)$, the relative L^1 -approximation error associated to $\mathbb{U}^{\Theta_m}(\xi)$, the uncorrected sample standard deviation of the relative approximation error associated to $\mathbb{U}^{\Theta_m}(\xi)$, the mean of the empirical loss function associated to $\mathbb{U}^{\Theta_m}(\xi)$, the standard deviation of the empirical loss function associated to $\mathbb{U}^{\Theta_m}(\xi)$, and the average runtime in seconds needed for calculating one realization of $\mathbb{U}^{\Theta_m}(\xi)$ against $m \in \{0, 500, 1000, 1500, 2000\}$ based on 10 independent realizations (10 independent runs). In addition, Figure 4 depicts approximations of the relative L^1 -approximation error and approximations of the mean of the empirical loss function associated to Θ_m against $m \in \{0, 1, \dots, 2000\}$ based on 10 independent realizations (10 independent runs). In the approximate calculations of the relative L^1 -approximation errors in Table 4 and Figure 4 the value $u(0, (0, 0, \dots, 0))$ of the solution u of the PDE (118) has been replaced by the value 0.09909 which, in turn, has been calculated through the Branching diffusion method (cf. MATLAB code 2 in Subsection A.2 below).

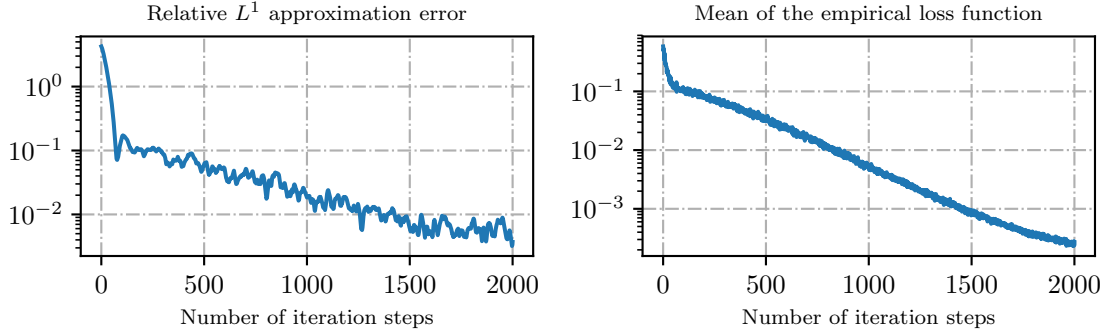


Figure 4: Plots of approximative calculations of the relative L^1 -approximation error $\mathbb{E}\left[\frac{|\mathbb{U}^{\Theta_m}(\xi) - 0.09909|}{0.09909}\right]$ and of the mean of the empirical loss function $\mathbb{E}\left[\frac{1}{J_m} \sum_{j=1}^{J_m} |\mathcal{Y}_N^{m, \Theta_m, j, \mathbb{S}_{m+1}} - g(\mathcal{X}_N^{m, j})|^2\right]$ in the case of the 50-dimensional Allen-Cahn equation (118) against $m \in \{0, 1, \dots, 2000\}$.

4.6 G -Brownian motions in 1 and 100 space-dimensions

In this subsection we use the deep 2BSDE method in Framework 3.2 to approximatively calculate nonlinear expectations of a test function on a 100-dimensional G -Brownian motion and of a test function on a 1-dimensional G -Brownian motion. In the case of the 100-dimensional G -Brownian motion we consider a specific test function such that the nonlinear expectation of this function on the 100-dimensional G -Brownian motion admits an explicit analytic solution (see Lemma 4.3 below). In the case of the 1-dimension G -Brownian motion we compare the numerical results of the deep 2BSDE method with numerical results obtained by a finite difference approximation method.

Assume the setting of Subsection 4.2, assume $T = 1$, $N = 20$, $\varepsilon = 10^{-8}$, let $\sigma_{\max} = 1$, $\sigma_{\min} = \frac{1}{\sqrt{2}}$, let $\bar{\sigma}: \mathbb{R} \rightarrow \mathbb{R}$ be the function which satisfies for all $x \in \mathbb{R}$ that

$$\bar{\sigma}(x) = \begin{cases} \sigma_{\max} & : x \geq 0 \\ \sigma_{\min} & : x < 0 \end{cases}, \quad (119)$$

assume for all $s, t \in [0, T]$, $x = (x_1, \dots, x_d)$, $w = (w_1, \dots, w_d)$, $z = (z_1, \dots, z_d) \in \mathbb{R}^d$, $y \in \mathbb{R}$, $S = (S_{ij})_{(i,j) \in \{1, \dots, d\}^2} \in \mathbb{R}^{d \times d}$ that $\sigma(x) = \text{Id}_{\mathbb{R}^d}$, $H(s, t, x, w) = x + w$, $g(x) = \|x\|_{\mathbb{R}^d}^2$, and

$$f(t, x, y, z, S) = -\frac{1}{2} \sum_{i=1}^d [\bar{\sigma}(S_{ii})]^2 S_{ii}. \quad (120)$$

The solution $u: [0, T] \times \mathbb{R}^d \rightarrow \mathbb{R}$ of the PDE (100) then satisfies for all $(t, x) \in [0, T] \times \mathbb{R}^d$

Number of iteration steps	Mean of \mathcal{U}^{Θ_m}	Standard deviation of \mathcal{U}^{Θ_m}	Rel. L^1 -approx. error	Standard deviation of the relative approx. error	Mean of the empirical loss function	Standard deviation of the empirical loss function	Runtime in sec. for one realiz. of \mathcal{U}^{Θ_m}
0	0.46	0.35878	0.99716	0.00221	26940.83	676.70	24
500	164.64	1.55271	0.01337	0.00929	13905.69	2268.45	757
1000	162.79	0.35917	0.00242	0.00146	1636.15	458.57	1491
1500	162.54	0.14143	0.00074	0.00052	403.00	82.40	2221

Table 5: Numerical simulations of the deep2BSDE method in Framework 3.2 in the case of the 100-dimensional G -Brownian motion (cf. (121) and (122)). In the approximative calculations of the relative L^1 -approximation errors the value $u(0, (1, 1/2, 1, 1/2, \dots, 1, 1/2))$ has been replaced by the value 162.5 which has been calculated by means of Lemma 4.3.

that $u(T, x) = g(x)$ and

$$\frac{\partial u}{\partial t}(t, x) + \frac{1}{2} \sum_{i=1}^d \left| \bar{\sigma} \left(\frac{\partial^2 u}{\partial x_i^2}(t, x) \right) \right|^2 \frac{\partial^2 u}{\partial x_i^2}(t, x) = 0. \quad (121)$$

In Table 5 we use an adapted version of PYTHON code 3 to approximatively calculate the mean $\mathbb{U}^{\Theta_m}(\xi)$, the standard deviation of $\mathbb{U}^{\Theta_m}(\xi)$, the relative L^1 -approximation error associated to $\mathbb{U}^{\Theta_m}(\xi)$, the uncorrected sample standard deviation of the relative approximation error associated to $\mathbb{U}^{\Theta_m}(\xi)$, the mean of the empirical loss function associated to $\mathbb{U}^{\Theta_m}(\xi)$, the standard deviation of the empirical loss function associated to $\mathbb{U}^{\Theta_m}(\xi)$, and the average runtime in seconds needed for calculating one realization of $\mathbb{U}^{\Theta_m}(\xi)$ against $m \in \{0, 500, 1000, 1500, 2000\}$ based on 10 realizations (10 independent runs) in the case where for all $x \in \mathbb{R}^d$, $m \in \mathbb{N}_0$, $\omega \in \Omega$ it holds that

$$d = 100, \quad g(x) = \|x\|_{\mathbb{R}^d}^2, \quad \gamma_m = \left[\frac{1}{2} \right]^{\lfloor \frac{m}{500} \rfloor}, \quad \text{and} \quad \xi(\omega) = (1, \frac{1}{2}, 1, \frac{1}{2}, \dots, 1, \frac{1}{2}) \in \mathbb{R}^d. \quad (122)$$

In addition, Figure 5 depicts approximations of the relative L^1 -approximation error associated to $\mathbb{U}^{\Theta_m}(\xi)$ and approximations of mean of the empirical loss function associated to Θ_m against $m \in \{0, 1, \dots, 2000\}$ based on 10 independent realizations (10 independent runs) in the case of (122). In the approximative calculations of the relative L^1 -approximation errors in Table 5 and Figure 5 the value $u(0, (1, 1/2, 1, 1/2, \dots, 1, 1/2))$ of the solution u of the PDE (cf. (121) and (122)) has been replaced by the value 162.5 which, in turn, has been calculated by means of Lemma 4.3 below (with $c = 1$, $\sigma_{\max} = 1$, $T = 1$, $\sigma_{\min} = 1/\sqrt{2}$, $d = 100$ in the notation of Lemma 4.3 below).

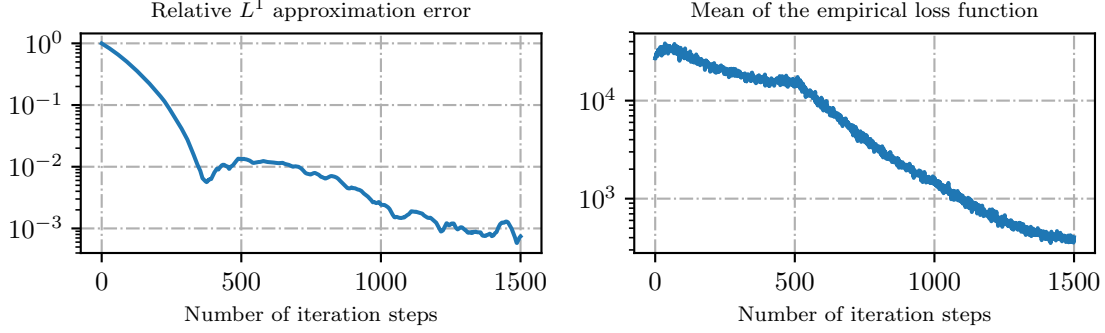


Figure 5: Plots of approximative calculations of the relative L^1 -approximation error $\mathbb{E} \left[\frac{|\mathbb{U}^{\Theta_m}(\xi) - 162.5|}{162.5} \right]$ and of the mean of the empirical loss function $\mathbb{E} \left[\frac{1}{J_m} \sum_{j=1}^{J_m} |\mathcal{Y}_N^{m, \Theta_m, j, \mathbb{S}_{m+1}} - g(\mathcal{X}_N^{m, j})|^2 \right]$ in the case of the 100-dimensional G -Brownian motion (cf. (121) and (122)) against $m \in \{0, 1, \dots, 1500\}$.

Lemma 4.3. *Let $c, \sigma_{\max}, T \in (0, \infty)$, $\sigma_{\min} \in (0, \sigma_{\max})$, $d \in \mathbb{N}$, let $\bar{\sigma}: \mathbb{R} \rightarrow \mathbb{R}$ be the function which satisfies for all $x \in \mathbb{R}$ that*

$$\bar{\sigma}(x) = \begin{cases} \sigma_{\max} & : x \geq 0 \\ \sigma_{\min} & : x < 0 \end{cases}, \quad (123)$$

and let $g: \mathbb{R}^d \rightarrow \mathbb{R}$ and $u: [0, T] \times \mathbb{R}^d \rightarrow \mathbb{R}$ be the functions which satisfy for all $t \in [0, T]$, $x = (x_1, \dots, x_d) \in \mathbb{R}^d$ that $g(x) = c\|x\|_{\mathbb{R}^d}^2 = c \sum_{i=1}^d |x_i|^2$ and

$$u(t, x) = g(x) + cd|\sigma_{\max}|^2(T - t). \quad (124)$$

Then it holds for all $t \in [0, T]$, $x = (x_1, \dots, x_d) \in \mathbb{R}^d$ that $u \in C^\infty([0, T] \times \mathbb{R}^d, \mathbb{R})$, $u(T, x) = g(x)$, and

$$\frac{\partial u}{\partial t}(t, x) + \frac{1}{2} \sum_{i=1}^d |\bar{\sigma}(\frac{\partial^2 u}{\partial x_i^2}(t, x))|^2 \frac{\partial^2 u}{\partial x_i^2}(t, x) = 0. \quad (125)$$

Proof of Lemma 4.3. Observe that the function u is clearly infinitely often differentiable. Next note that (124) ensures that for all $t \in [0, T]$, $x = (x_1, \dots, x_d) \in \mathbb{R}^d$, $i \in \{1, 2, \dots, d\}$ it holds that

$$\frac{\partial u}{\partial t}(t, x) = \frac{\partial}{\partial t} [g(x) + cd|\sigma_{\max}|^2(T - t)] = \frac{\partial}{\partial t} [cd|\sigma_{\max}|^2(T - t)] = -cd|\sigma_{\max}|^2 \quad (126)$$

and

$$\frac{\partial^2 u}{\partial x_i^2}(t, x) = \frac{\partial^2}{\partial x_i^2} [g(x) + cd|\sigma_{\max}|^2(T - t)] = \frac{\partial^2 g}{\partial x_i^2}(x) = 2c > 0. \quad (127)$$

Number of iteration steps	Mean of \mathcal{U}^{Θ_m}	Standard deviation of \mathcal{U}^{Θ_m}	Rel. L^1 -approx. error	Standard deviation of the relative approx. error	Mean of the empirical loss function	Standard deviation of the empirical loss function	Runtime in sec. for one realiz. of \mathcal{U}^{Θ_m}
0	0.4069	0.28711	0.56094	0.29801	29.905	25.905	22
100	0.8621	0.07822	0.08078	0.05631	1.003	0.593	24
200	0.9097	0.01072	0.00999	0.00840	0.159	0.068	26
300	0.9046	0.00320	0.00281	0.00216	0.069	0.048	28
500	0.9017	0.00159	0.00331	0.00176	0.016	0.005	32

Table 6: Numerical simulations of the deep2BSDE method in Framework 3.2 in the case of the 1-dimensional G -Brownian motion (cf. (121) and (130)). In the approximative calculations of the relative L^1 -approximation error the value $u(0, -2)$ has been replaced by the value 0.90471 which has been calculated through finite differences approximations (cf. MATLAB code 5 in Subsection A.5 below).

Combining this with (123) shows that for all $t \in [0, T]$, $x = (x_1, \dots, x_d) \in \mathbb{R}^d$, $i \in \{1, 2, \dots, d\}$ it holds that

$$\bar{\sigma}\left(\frac{\partial^2 u}{\partial x_i^2}(t, x)\right) = \bar{\sigma}(2c) = \sigma_{\max}. \quad (128)$$

This, (126), and (127) yield that for all $t \in [0, T]$, $x = (x_1, \dots, x_d) \in \mathbb{R}^d$ it holds that

$$\begin{aligned} \frac{\partial u}{\partial t}(t, x) + \frac{1}{2} \sum_{i=1}^d \left| \bar{\sigma}\left(\frac{\partial^2 u}{\partial x_i^2}(t, x)\right) \right|^2 \frac{\partial^2 u}{\partial x_i^2}(t, x) &= \frac{\partial u}{\partial t}(t, x) + \frac{1}{2} \sum_{i=1}^d |\sigma_{\max}|^2 \frac{\partial^2 u}{\partial x_i^2}(t, x) \\ &= \frac{\partial u}{\partial t}(t, x) + cd|\sigma_{\max}|^2 = 0. \end{aligned} \quad (129)$$

This completes the proof of Lemma 4.3. □

In Table 6 we use an adapted version of PYTHON code 3 in Subsection A.3 below to approximatively calculate the mean of $\mathbb{U}^{\Theta_m}(\xi)$, the standard deviation of $\mathbb{U}^{\Theta_m}(\xi)$, the relative L^1 -approximation error associated to $\mathbb{U}^{\Theta_m}(\xi)$, the uncorrected sample standard deviation of the relative approximation error associated to $\mathbb{U}^{\Theta_m}(\xi)$, the mean of the empirical loss function associated to $\mathbb{U}^{\Theta_m}(\xi)$, the standard deviation of the empirical loss function associated to $\mathbb{U}^{\Theta_m}(\xi)$, and the average runtime in seconds needed for calculating one realization of $\mathbb{U}^{\Theta_m}(\xi)$ against $m \in \{0, 100, 200, 300, 500\}$ based on 10 realizations (10 independent runs) in the case where for all $x \in \mathbb{R}^d$, $m \in \mathbb{N}_0$, $\omega \in \Omega$ it holds that

$$d = 1, \quad g(x) = \frac{1}{1 + \exp(-x^2)}, \quad \gamma_m = \frac{1}{100}, \quad \text{and} \quad \xi(\omega) = -2. \quad (130)$$

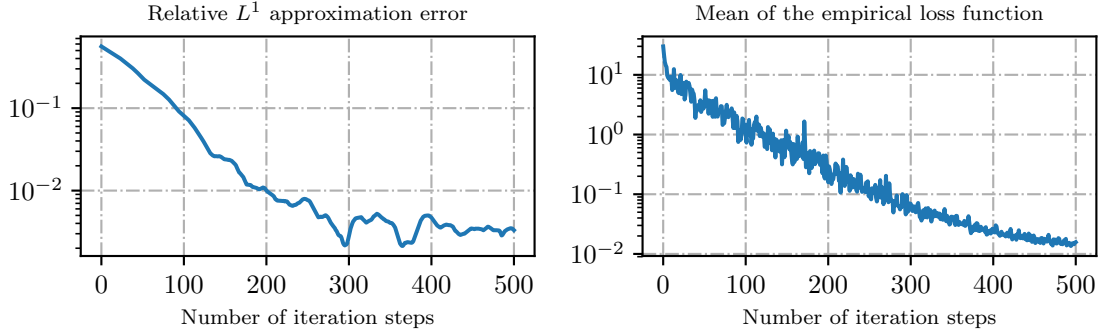


Figure 6: Plots of approximative calculations of the relative L^1 -approximation error $\mathbb{E}\left[\frac{|\mathbb{U}^{\Theta_m}(\xi)-0.90471|}{0.90471}\right]$ and of the mean of the empirical loss function $\mathbb{E}\left[\frac{1}{J_m} \sum_{j=1}^{J_m} |\mathcal{Y}_N^{m, \Theta_m, j, \mathbb{S}_{m+1}} - g(\mathcal{X}_N^{m, j})|^2\right]$ in the case of the 1-dimensional G -Brownian motion (cf. (121) and (130)) against $m \in \{0, 1, \dots, 500\}$.

In addition, Figure 6 depicts approximations of the relative L^1 -approximation error associated to $\mathbb{U}^{\Theta_m}(\xi)$ and approximations of the mean of empirical loss function associated to Θ_m for $m \in \{0, 1, \dots, 500\}$ based on 10 independent realizations (10 independent runs) in the case of (130). In the approximative calculations of the relative L^1 -approximation errors in Table 5 and Figure 5 the value $u(0, -2)$ of the solution u of the PDE (cf. (121) and (130)) has been replaced by the value 0.90471 which, in turn, has been calculated by means of finite differences approximations (cf. MATLAB code 5 in Subsection A.5 below).

A Source codes

A.1 A PYTHON code for the deep 2BSDE method used in Subsection 4.1

The following PYTHON code, PYTHON code 1 below, is a simplified version of PYTHON code 3 in Subsection A.3 below.

```

1  #!/usr/bin/python3
2
3  """
4  Plain deep2BSDE solver with hard-coded Allen-Cahn equation
5  """
6
7  import tensorflow as tf
8  import numpy as np
9  import time, datetime
10

```

```

11 tf.reset_default_graph()
12 start_time = time.time()
13
14 name = 'AllenCahn'
15
16 # setting of the problem
17 d = 20
18 T = 0.3
19 Xi = np.zeros([1,d])
20
21 # setup of algorithm and implementation
22 N = 20
23 h = T/N
24 sqrth = np.sqrt(h)
25 n_maxstep = 10000
26 batch_size = 1
27 gamma = 0.001
28
29 # neural net architectures
30 n_neuronForGamma = [d, d, d, d**2]
31 n_neuronForA = [d, d, d, d]
32
33 # (adapted) rhs of the pde
34 def f0(t,X,Y,Z,Gamma):
35     return -Y+tf.pow(Y, 3)
36
37 # terminal condition
38 def g(X):
39     return 1/(1 + 0.2*tf.reduce_sum(tf.square(X),
40                                     1, keep_dims=True))*0.5
41
42 # helper functions for constructing the neural net(s)
43 def _one_time_net(x, name, isgamma = False):
44     with tf.variable_scope(name):
45         layer1 = _one_layer(x, (1-isgamma)*n_neuronForA[1] \
46                             +isgamma*n_neuronForGamma[1], name = 'layer1')
47         layer2 = _one_layer(layer1, (1-isgamma)*n_neuronForA[2] \
48                             +isgamma*n_neuronForGamma[2], name = 'layer2')
49         z = _one_layer(layer2, (1-isgamma)*n_neuronForA[3] \
50                         +isgamma*n_neuronForGamma[3], activation_fn=None,
51                         name = 'final')
52     return z
53
54 def _one_layer(input_, output_size, activation_fn=tf.nn.relu,
55               stddev=5.0, name='linear'):
56     with tf.variable_scope(name):
57         shape = input_.get_shape().as_list()
58         w = tf.get_variable('Matrix', [shape[1], output_size],
59                             tf.float64,

```

```

60         tf.random_normal_initializer(
61             stddev=stddev/np.sqrt(shape[1]+output_size)))
62     b = tf.get_variable('Bias', [1,output_size], tf.float64,
63         tf.constant_initializer(0.0))
64     hidden = tf.matmul(input_, w) + b
65     if activation_fn:
66         return activation_fn(hidden)
67     else:
68         return hidden
69
70 with tf.Session() as sess:
71     # background dynamics
72     dW = tf.random_normal(shape=[batch_size, d], stddev = sqrth,
73         dtype=tf.float64)
74
75     # initial values of the stochastic processes
76     X = tf.Variable(np.ones([batch_size, d]) * Xi,
77         dtype = tf.float64,
78         name='X',
79         trainable=False)
80     Y0 = tf.Variable(tf.random_uniform([1],
81         minval = -1, maxval = 1,
82         dtype=tf.float64),
83         name='Y0')
84     Z0 = tf.Variable(tf.random_uniform([1,d],
85         minval = -.1, maxval = .1,
86         dtype=tf.float64),
87         name='Z0')
88     Gamma0 = tf.Variable(tf.random_uniform([d, d],
89         minval = -.1, maxval = .1,
90         dtype=tf.float64),
91         name='Gamma0')
92     A0 = tf.Variable(tf.random_uniform([1,d],
93         minval = -.1, maxval = .1,
94         dtype=tf.float64),
95         name='A0')
96     allones = tf.ones(shape=[batch_size, 1],
97         dtype=tf.float64,
98         name='MatrixOfOnes')
99     Y = allones * Y0
100    Z = tf.matmul(allones,Z0)
101    Gamma = tf.multiply(tf.ones([batch_size, d, d],
102        dtype = tf.float64), Gamma0)
103    A = tf.matmul(allones,A0)
104
105    # forward discretization
106    with tf.variable_scope('forward'):
107        for i in range(N-1):
108            Y = Y + f0(i*h,X,Y,Z,Gamma)*h \

```

```

109         + tf.reduce_sum(dW*Z, 1, keep_dims=True)
110     Z = Z + A * h \
111         + tf.squeeze(tf.matmul(Gamma,
112                               tf.expand_dims(dW, -1)))
113     Gamma = tf.reshape(_one_time_net(X, name=str(i)+'Gamma',
114                                   isgamma=True)/d**2,
115                       [batch_size, d, d])
116     if i!=N-1:
117         A = _one_time_net(X, name=str(i)+'A')/d
118     X = X + dW
119     dW = tf.random_normal(shape=[batch_size, d],
120                           stddev = sqrth, dtype=tf.float64)
121
122     Y = Y + f0( (N-1)*h , X,Y,Z,Gamma)*h \
123         + tf.reduce_sum(dW*Z, 1, keep_dims=True)
124     X = X + dW
125     loss_function = tf.reduce_mean(tf.square(Y-g(X)))
126
127     # specifying the optimizer
128     global_step = tf.get_variable('global_step', [],
129                                   initializer=tf.constant_initializer(0),
130                                   trainable=False, dtype=tf.int32)
131
132     learning_rate = tf.train.exponential_decay(gamma, global_step,
133                                               decay_steps = 10000, decay_rate = 0.0, staircase = True)
134
135     trainable_variables = tf.trainable_variables()
136     grads = tf.gradients(loss_function, trainable_variables)
137     optimizer = tf.train.GradientDescentOptimizer(
138         learning_rate=learning_rate)
139     apply_op = optimizer.apply_gradients(
140         zip(grads, trainable_variables),
141         global_step=global_step, name='train_step')
142
143     with tf.control_dependencies([apply_op]):
144         train_op_2 = tf.identity(loss_function, name='train_op2')
145
146     # to save history
147     learning_rates = []
148     y0_values = []
149     losses = []
150     running_time = []
151     steps = []
152     sess.run(tf.global_variables_initializer())
153
154     try:
155         # the actual training loop
156         for _ in range(n_maxstep + 1):
157             y0_value, step = sess.run([Y0, global_step])

```

```

158         currentLoss, currentLearningRate = sess.run(
159             [train_op_2, learning_rate])
160
161         learning_rates.append(currentLearningRate)
162         losses.append(currentLoss)
163         y0_values.append(y0_value)
164         running_time.append(time.time()-start_time)
165         steps.append(step)
166
167         if step % 100 == 0:
168             print("step: ", step,
169                 " loss: ", currentLoss,
170                 " Y0: " , y0_value,
171                 " learning rate: ", currentLearningRate)
172
173         end_time = time.time()
174         print("running time: ", end_time-start_time)
175
176     except KeyboardInterrupt:
177         print("\nmanually disengaged")
178
179     # writing results to a csv file
180     output = np.zeros((len(y0_values),5))
181     output[:,0] = steps
182     output[:,1] = losses
183     output[:,2] = y0_values
184     output[:,3] = learning_rates
185     output[:,4] = running_time
186
187     np.savetxt("./" + str(name) + "_d" + str(d) + "_" + \
188         datetime.datetime.now().strftime('%Y-%m-%d-%H:%M:%S')+ ".csv",
189         output,
190         delimiter = ",",
191         header = "step, loss function, Y0, learning rate, running time",
192         )

```

PYTHON code 1: A PYTHON code for the deep 2BSDE method used in Subsection 4.1. This PYTHON code uses the plain stochastic gradient descent method and does not use batch normalization.

A.2 A MATLAB code for the Branching diffusion method used in Subsection 4.1

The following MATLAB code is a slightly modified version of the MATLAB code in E, Han, & Jentzen [33, Subsection 6.2].

```

1 function Branching()
2     rng('default');
3
4 % Parameter
5     T = 0.3;
6     M = 10^7;
7     t0 = 0;
8
9     d = 20; m = d;
10    beta = 1;
11    mu = zeros(d,1);
12    sigma = eye(d);
13    a = [0 2 0 -1]';
14    p = [0 0.5 0 0.5]';
15    psi = @(x) 1./(1+0.2*norm(x)^2)*1/2;
16    x0 = 0;
17
18 % Branching PDE Solver
19    tic;
20    [result,SD] = ...
21        MCBranchingEvaluation(...
22            mu, sigma, beta, p, a, t0, x0, T, psi, M);
23    runtime = toc;
24    disp(['BranchingP solver: u(0,x0) = ' num2str(result) '']);
25    disp(['Runtime = ' num2str(runtime) '']);
26 end
27
28 function [result,SD] = ...
29 MCBranchingEvaluation(...
30     mu, sigma, beta, p, a, t0, x0, T, psi, M)
31     result = 0;
32     SD = 0;
33     for m=1:M
34         Evl = BranchingEvaluation(...
35             mu, sigma, beta, p, a, t0, x0, T, psi);
36         result = result + Evl;
37         SD = SD + Evl^2;
38     end
39     SD = sqrt( (SD - result^2/M)/M );
40     result = result/M;
41 end
42
43 function Evl = ...
44 BranchingEvaluation(...
45     mu, sigma, beta, p, a, t0, x0, T, psi)
46     BP = BranchingProcess(mu, sigma, beta, p, t0, x0, T);
47     Evl = 1;
48     for k=1:size(BP{1},2)
49         Evl = Evl * psi( BP{1}(:,k) );

```

```

50     end
51     if norm(a-p) > 0
52         for k=1:length(a)
53             if p(k) > 0
54                 Evl = Evl * ( a(k)/p(k) )^( BP{2}(k) );
55             elseif a(k) ~= 0
56                 error('a(k) zero but p(k) non-zero');
57             end
58         end
59     end
60 end

61
62 function BP = ...
63 BranchingProcess(mu, sigma, beta, p, t0, x0, T)
64     BP = cell(2,1);
65     BP{2} = p*0;
66     tau = exprnd(1/beta);
67     new_t0 = min( tau + t0, T );
68     delta_t = new_t0 - t0;
69     m = size(sigma,2);
70     new_x0 = x0 + mu*delta_t + sigma*sqrt(delta_t)*randn(m,1);
71     if tau >= T - t0
72         BP{1} = new_x0;
73     else
74         [tmp,which_nonlinearity] = max(mnrnd(1,p));
75         BP{2}(which_nonlinearity) = BP{2}(which_nonlinearity) + 1;
76         for k=1:which_nonlinearity-1
77             tmp = BranchingProcess(...
78                 mu, sigma, beta, p, new_t0, new_x0, T);
79             BP{1} = [ BP{1} tmp{1} ];
80             BP{2} = BP{2} + tmp{2};
81         end
82     end
83 end

```

MATLAB code 2: A MATLAB code for the Branching diffusion method used in Subsection 4.5.

A.3 A PYTHON code for the deep 2BSDE method used in Subsection 4.3

The following PYTHON code is based on the PYTHON code in E, Han, & Jentzen [33, Subsection 6.1].

```

1  #!/usr/bin/python3
2  # -*- coding: utf-8 -*-
3

```



```

4  """
5  Deep2BSDE solver with hard-coded Black-Scholes-Barenblatt equation.
6  """
7
8  import time, datetime
9  import tensorflow as tf
10 import numpy as np
11 from tensorflow.python.training import moving_averages
12
13 start_time = time.time()
14 tf.reset_default_graph()
15
16 name = 'BSB'
17 d = 100
18 batch_size = 64
19 T = 1.0
20 N = 20
21 h = T/N
22 sqrth = np.sqrt(h)
23 n_maxstep = 500
24 n_displaystep = 100
25 n_neuronForA = [d,d,d,d]
26 n_neuronForGamma = [d,d,d,d**2]
27 Xinit = np.array([1.0,0.5]*50)
28 mu = 0
29 sigma = 0.4
30 sigma_min = 0.1
31 sigma_max = 0.4
32 r = 0.05
33
34 _extra_train_ops = []
35
36 def sigma_value(W):
37     return sigma_max * \
38         tf.cast(tf.greater_equal(W, tf.cast(0,tf.float64)),
39               tf.float64) + \
40         sigma_min * tf.cast(tf.greater(tf.cast(0,tf.float64), W),
41                             tf.float64)
42
43 def f_tf(t, X, Y, Z, Gamma):
44     return -0.5*tf.expand_dims(tf.trace(
45         tf.square(tf.expand_dims(X,-1)) * \
46         (tf.square(sigma_value(Gamma))-sigma**2) * Gamma),-1) + \
47         r * (Y - tf.reduce_sum(X*Z, 1, keep_dims = True))
48
49 def g_tf(X):
50     return tf.reduce_sum(tf.square(X),1, keep_dims = True)
51
52 def sigma_function(X):

```

```

53     return sigma * tf.matrix_diag(X)
54
55 def mu_function(X):
56     return mu * X
57
58 def _one_time_net(x, name, isgamma = False):
59     with tf.variable_scope(name):
60         x_norm = _batch_norm(x, name='layer0_normalization')
61         layer1 = _one_layer(x_norm, (1-isgamma)*n_neuronForA[1] \
62             +isgamma*n_neuronForGamma[1], name = 'layer1')
63         layer2 = _one_layer(layer1, (1-isgamma)*n_neuronForA[2] \
64             +isgamma*n_neuronForGamma[2], name = 'layer2')
65         z = _one_layer(layer2, (1-isgamma)*n_neuronForA[3] \
66             +isgamma*n_neuronForGamma[3], activation_fn=None,
67             name = 'final')
68     return z
69
70 def _one_layer(input_, output_size, activation_fn=tf.nn.relu,
71               stddev=5.0, name='linear'):
72     with tf.variable_scope(name):
73         shape = input_.get_shape().as_list()
74         w = tf.get_variable('Matrix', [shape[1], output_size],
75                             tf.float64,
76                             tf.random_normal_initializer(
77                                 stddev=stddev/np.sqrt(shape[1]+output_size)))
78         hidden = tf.matmul(input_, w)
79         hidden_bn = _batch_norm(hidden, name='normalization')
80     if activation_fn:
81         return activation_fn(hidden_bn)
82     else:
83         return hidden_bn
84
85 def _batch_norm(x, name):
86     """Batch normalization"""
87     with tf.variable_scope(name):
88         params_shape = [x.get_shape()[-1]]
89         beta = tf.get_variable('beta', params_shape, tf.float64,
90                               initializer=tf.random_normal_initializer(
91                                   0.0, stddev=0.1, dtype=tf.float64))
92         gamma = tf.get_variable('gamma', params_shape, tf.float64,
93                                 initializer=tf.random_uniform_initializer(
94                                     0.1, 0.5, dtype=tf.float64))
95         moving_mean = tf.get_variable('moving_mean',
96                                       params_shape, tf.float64,
97                                       initializer=tf.constant_initializer(0.0, tf.float64),
98                                       trainable=False)
99         moving_variance = tf.get_variable('moving_variance',
100                                         params_shape, tf.float64,
101                                         initializer=tf.constant_initializer(1.0, tf.float64),

```

```

102         trainable=False)
103     mean, variance = tf.nn.moments(x, [0], name='moments')
104     _extra_train_ops.append(
105         moving_averages.assign_moving_average(
106             moving_mean, mean, 0.99))
107     _extra_train_ops.append(
108         moving_averages.assign_moving_average(
109             moving_variance, variance, 0.99))
110     y = tf.nn.batch_normalization(
111         x, mean, variance, beta, gamma, 1e-6)
112     y.set_shape(x.get_shape())
113     return y
114
115 with tf.Session() as sess:
116
117     dW = tf.random_normal(shape=[batch_size, d],
118                           stddev = 1, dtype=tf.float64)
119     X = tf.Variable(np.ones([batch_size, d]) * Xinit,
120                   dtype=tf.float64,
121                   trainable=False)
122     Y0 = tf.Variable(tf.random_uniform(
123         [1],
124         minval=0, maxval=1, dtype=tf.float64),
125                    name='Y0');
126     Z0 = tf.Variable(tf.random_uniform(
127         [1, d],
128         minval=-.1, maxval=.1,
129         dtype=tf.float64),
130                    name='Z0')
131     Gamma0 = tf.Variable(tf.random_uniform(
132         [d, d],
133         minval=-1, maxval=1,
134         dtype=tf.float64), name='Gamma0')
135     A0 = tf.Variable(tf.random_uniform(
136         [1, d], minval=-.1, maxval=.1,
137         dtype=tf.float64), name='A0')
138     allones = tf.ones(shape=[batch_size, 1], dtype=tf.float64,
139                      name='MatrixOfOnes')
140     Y = allones * Y0
141     Z = tf.matmul(allones, Z0)
142     A = tf.matmul(allones, A0)
143     Gamma = tf.multiply(tf.ones(shape=[batch_size, d, d],
144                                dtype=tf.float64), Gamma0)
145     with tf.variable_scope('forward'):
146         for t in range(0, N-1):
147             # Y update inside the loop
148             dX = mu * X * h + sqrth * sigma * X * dW
149             Y = Y + f_tf(t * h, X, Y, Z, Gamma)*h \
150                 + tf.reduce_sum(Z*dX, 1, keep_dims = True)

```

```

151     X = X + dX
152     # Z update inside the loop
153     Z = Z + A * h \
154         + tf.squeeze(tf.matmul(Gamma,
155                                tf.expand_dims(dX, -1),
156                                transpose_b=False))
157     A = _one_time_net(X, str(t+1)+"A" )/d
158     Gamma = _one_time_net(X, str(t+1)+"Gamma",
159                           isgamma = True)/d**2
160     Gamma = tf.reshape(Gamma, [batch_size, d, d])
161     dW = tf.random_normal(shape=[batch_size, d],
162                           stddev = 1, dtype=tf.float64)
163     # Y update outside of the loop - terminal time step
164     dX = mu * X * h + sqrth * sigma * X * dW
165     Y = Y + f_tf((N-1) * h, X, Y, Z, Gamma)*h \
166         + tf.reduce_sum(Z * dX, 1, keep_dims=True)
167     X = X + dX
168     loss = tf.reduce_mean(tf.square(Y-g_tf(X)))
169
170     # training operations
171     global_step = tf.get_variable('global_step', [],
172                                   initializer=tf.constant_initializer(0),
173                                   trainable=False, dtype=tf.int32)
174
175     learning_rate = tf.train.exponential_decay(1.0, global_step,
176                                               decay_steps = 200,
177                                               decay_rate = 0.5,
178                                               staircase=True)
179
180     trainable_variables = tf.trainable_variables()
181     grads = tf.gradients(loss, trainable_variables)
182     optimizer = tf.train.AdamOptimizer(
183         learning_rate=learning_rate
184     )
185     apply_op = optimizer.apply_gradients(
186         zip(grads, trainable_variables),
187         global_step=global_step, name='train_step')
188     train_ops = [apply_op] + _extra_train_ops
189     train_op = tf.group(*train_ops)
190
191     with tf.control_dependencies([train_op]):
192         train_op_2 = tf.identity(loss, name='train_op2')
193
194     # to save history
195     learning_rates = []
196     y0_values = []
197     losses = []
198     running_time = []
199     steps = []

```

```

200     sess.run(tf.global_variables_initializer())
201
202     try:
203
204         for _ in range(n_maxstep+1):
205             step, y0_value = sess.run([global_step, Y0])
206             currentLoss, currentLearningRate = sess.run(
207                 [train_op_2, learning_rate])
208
209             steps.append(step)
210             losses.append(currentLoss)
211             y0_values.append(y0_value)
212             learning_rates.append(currentLearningRate)
213             running_time.append(time.time()-start_time)
214
215             if step % n_displaystep == 0:
216                 print("step: ", step,
217                     " loss: ", currentLoss,
218                     " Y0: ", y0_value,
219                     " learning rate: ", currentLearningRate)
220
221             end_time = time.time()
222             print("running time: ", end_time-start_time)
223
224         except KeyboardInterrupt:
225             print("manually disengaged")
226
227     # writing results to a csv file
228     output = np.zeros((len(y0_values),5))
229     output[:,0] = steps
230     output[:,1] = losses
231     output[:,2] = y0_values
232     output[:,3] = learning_rates
233     output[:,4] = running_time
234     np.savetxt("./" + str(name) + "_d" + str(d) + "_" + \
235               datetime.datetime.now().strftime('%Y-%m-%d-%H:%M:%S') + ".csv",
236               output,
237               delimiter = ",",
238               header = "step, loss function, Y0, learning rate, running time"
239               )

```

PYTHON code 3: A PYTHON code for the deep 2BSDE method used in Subsection 4.3.

A.4 A MATLAB code for the classical Monte Carlo method used in Subsection 4.4

The following MATLAB code is a slightly modified version of the MATLAB code in E, Han, & Jentzen [33, Subsection 6.3].

```
1 rng('default');
2 M = 10^7;
3 d = 100;
4 MC = 0;
5 for m=1:M
6     dW = randn(1,d);
7     MC = MC + 2/(1+norm(sqrt(2)*dW)^2);
8 end
9 MC = -log(MC/M);
```

MATLAB code 4: A MATLAB code for the classical Monte Carlo method used in Subsection 4.4.

A.5 A MATLAB code for the finite differences method used in Subsection 4.6

The following MATLAB code is inspired by the MATLAB code in E et al. [35, MATLAB code 7 in Section 3].

```
1 function GBrownianMotion()
2     disp(num2str(finiteDiff_GBrownianMotion(0,-2,1000)))
3 end
4
5 function y = finiteDiff_GBrownianMotion(t0,x0,N)
6     sigma_max = 1.0;
7     sigma_min = 0.5;
8     T = 1.0;
9     sigma = 1;
10    f = @(t,x,y,z,gamma) 0.5 * ((gamma>0).*sigma_max ...
11        + (gamma<=0).*sigma_min).* gamma;
12
13    g = @(x) 1./(1+exp(-x.^2));
14    h=(T-t0)./N;
15    t=t0:h:T;
16    d1 = 0.05;
17    d2=sigma*d1;
18    x=x0+d1*(-N:1:N);
19    M=(1/(h))*[[1, zeros(1,2.*N-2)];
20        full/gallery('tridiag',...
21            ones(2.*N-2,1),-2*ones(2.*N-1,1),ones(2.*N-2,1)));
22        [zeros(1,2*N-2),1]]];
```

```

23     L=1/(2*d1)*([-1, zeros(1,2.*N-2)];
24                full/gallery('tridiag',...
25                             ones(2.*N-2,1),zeros(2.*N-1,1),-ones(2.*N-2,1)));
26                [zeros(1,2*N-2),1]);
27     y=g(x);
28     for i=N:-1:1
29         x=x(1:(2*i-1))+d2;
30         tmp = y(2:(2*i));
31         z=y*L(1:(2*i+1),1:(2*i-1));
32         gamma=y*M(1:(2*i+1),1:(2*i-1));
33         y=tmp+h*f(t(i),x,tmp,z,gamma);
34     end
35 end

```

MATLAB code 5: A MATLAB code for the finite differences method used in Subsection 4.6.

Acknowledgements

Sebastian Becker and Jiequn Han are gratefully acknowledged for their helpful and inspiring comments regarding the implementation of the deep 2BSDE method.

References

- [1] AMADORI, A. L. Nonlinear integro-differential evolution problems arising in option pricing: a viscosity solutions approach. *Differential Integral Equations* 16, 7 (2003), 787–811.
- [2] AVELLANEDA, M., , A. L., AND PARÁS, A. Pricing and hedging derivative securities in markets with uncertain volatilities. *Appl. Math. Finance* 2, 2 (1995), 73–88.
- [3] BALLY, V., AND PAGÈS, G. A quantization algorithm for solving multi-dimensional discrete-time optimal stopping problems. *Bernoulli* 9, 6 (2003), 1003–1049.
- [4] BAYRAKTAR, E., MILEVSKY, M. A., PROMISLOW, S. D., AND YOUNG, V. R. Valuation of mortality risk via the instantaneous Sharpe ratio: applications to life annuities. *J. Econom. Dynam. Control* 33, 3 (2009), 676–691.
- [5] BAYRAKTAR, E., AND YOUNG, V. Pricing options in incomplete equity markets via the instantaneous sharpe ratio. *Ann. Finance* 4, 4 (2008), 399–429.
- [6] BENDER, C., AND DENK, R. A forward scheme for backward SDEs. *Stochastic Process. Appl.* 117, 12 (2007), 1793–1812.
- [7] BENDER, C., SCHWEIZER, N., AND ZHUO, J. A primal-dual algorithm for BSDEs. *Math. Finance* 27, 3 (2017), 866–901.
- [8] BENGIO, Y. Learning deep architectures for AI. *Foundations and Trends in Machine Learning* 2, 1 (2009), 1–127.
- [9] BERGMAN, Y. Z. Option pricing with differential interest rates. *The Review of Financial Studies* 8, 2 (1995), 475–500.
- [10] BISMUT, J.-M. Conjugate convex functions in optimal stochastic control. *J. Math. Anal. Appl.* 44 (1973), 384–404.
- [11] BOUCHARD, B. *Lecture notes on BSDEs: Main existence and stability results*. PhD thesis, CEREMADE-Centre de Recherches en MATHématiques de la DEcision, 2015.
- [12] BOUCHARD, B., ELIE, R., AND TOUZI, N. Discrete-time approximation of BSDEs and probabilistic schemes for fully nonlinear PDEs. In *Advanced financial modelling*, vol. 8 of *Radon Ser. Comput. Appl. Math.* Walter de Gruyter, Berlin, 2009, pp. 91–124.
- [13] BOUCHARD, B., AND TOUZI, N. Discrete-time approximation and Monte-Carlo simulation of backward stochastic differential equations. *Stochastic Process. Appl.* 111, 2 (2004), 175–206.

- [14] BRIAND, P., AND LABART, C. Simulation of BSDEs by Wiener chaos expansion. *Ann. Appl. Probab.* 24, 3 (2014), 1129–1171.
- [15] CAI, Z. Approximating quantum many-body wave-functions using artificial neural networks. *arXiv:1704.05148* (2017), 8 pages.
- [16] CARLEO, G., AND TROYER, M. Solving the quantum many-body problem with artificial neural networks. *Science* 355, 6325 (2017), 602–606.
- [17] CHANG, D., LIU, H., AND XIONG, J. A branching particle system approximation for a class of FBSDEs. *Probab. Uncertain. Quant. Risk* 1 (2016), Paper No. 9, 34.
- [18] CHASSAGNEUX, J.-F. Linear multistep schemes for BSDEs. *SIAM J. Numer. Anal.* 52, 6 (2014), 2815–2836.
- [19] CHASSAGNEUX, J.-F., AND CRISAN, D. Runge-Kutta schemes for backward stochastic differential equations. *Ann. Appl. Probab.* 24, 2 (2014), 679–720.
- [20] CHASSAGNEUX, J.-F., AND RICHOU, A. Numerical stability analysis of the Euler scheme for BSDEs. *SIAM J. Numer. Anal.* 53, 2 (2015), 1172–1193.
- [21] CHASSAGNEUX, J.-F., AND RICHOU, A. Numerical simulation of quadratic BSDEs. *Ann. Appl. Probab.* 26, 1 (2016), 262–304.
- [22] CHERIDITO, P., SONER, H. M., TOUZI, N., AND VICTOIR, N. Second-order backward stochastic differential equations and fully nonlinear parabolic PDEs. *Comm. Pure Appl. Math.* 60, 7 (2007), 1081–1110.
- [23] CHIARAMONTE, M., AND KIENER, M. Solving differential equations using neural networks. *Machine Learning Project*, 5 pages.
- [24] CRÉPEY, S., GERBOUD, R., GRBAC, Z., AND NGOR, N. Counterparty risk and funding: the four wings of the TVA. *Int. J. Theor. Appl. Finance* 16, 2 (2013), 1350006, 31.
- [25] CRISAN, D., AND MANOLARAKIS, K. Probabilistic methods for semilinear partial differential equations. Applications to finance. *M2AN Math. Model. Numer. Anal.* 44, 5 (2010), 1107–1133.
- [26] CRISAN, D., AND MANOLARAKIS, K. Solving backward stochastic differential equations using the cubature method: application to nonlinear pricing. *SIAM J. Financial Math.* 3, 1 (2012), 534–571.
- [27] CRISAN, D., AND MANOLARAKIS, K. Second order discretization of backward SDEs and simulation with the cubature method. *Ann. Appl. Probab.* 24, 2 (2014), 652–678.

- [28] CRISAN, D., MANOLARAKIS, K., AND TOUZI, N. On the Monte Carlo simulation of BSDEs: an improvement on the Malliavin weights. *Stochastic Process. Appl.* 120, 7 (2010), 1133–1158.
- [29] DARBON, J., AND OSHER, S. Algorithms for overcoming the curse of dimensionality for certain Hamilton-Jacobi equations arising in control theory and elsewhere. *Res. Math. Sci.* 3 (2016), Paper No. 19, 26.
- [30] DEHGHAN, M., NOURIAN, M., AND MENHAJ, M. B. Numerical solution of Helmholtz equation by the modified Hopfield finite difference techniques. *Numer. Methods Partial Differential Equations* 25, 3 (2009), 637–656.
- [31] DELARUE, F., AND MENOZZI, S. A forward-backward stochastic algorithm for quasi-linear PDEs. *Ann. Appl. Probab.* 16, 1 (2006), 140–184.
- [32] DOUGLAS, JR., J., MA, J., AND PROTTER, P. Numerical methods for forward-backward stochastic differential equations. *Ann. Appl. Probab.* 6, 3 (1996), 940–968.
- [33] E, W., HAN, J., AND JENTZEN, A. Deep learning-based numerical methods for high-dimensional parabolic partial differential equations and backward stochastic differential equations. *arXiv:1706.04702* (2017), 39 pages.
- [34] E, W., HUTZENTHALER, M., JENTZEN, A., AND KRUSE, T. Linear scaling algorithms for solving high-dimensional nonlinear parabolic differential equations. *arXiv:1607.03295* (2017), 18 pages.
- [35] E, W., HUTZENTHALER, M., JENTZEN, A., AND KRUSE, T. On multilevel picard numerical approximations for high-dimensional nonlinear parabolic partial differential equations and high-dimensional nonlinear backward stochastic differential equations. *arXiv:1708.03223* (2017), 25 pages.
- [36] EKREN, I., AND MUHLE-KARBE, J. Portfolio choice with small temporary and transient price impact. *arXiv:1705.00672* (2017), 42 pages.
- [37] EL KAROUI, N., PENG, S., AND QUENEZ, M. C. Backward stochastic differential equations in finance. *Math. Finance* 7, 1 (1997), 1–71.
- [38] FAHIM, A., TOUZI, N., AND WARIN, X. A probabilistic numerical method for fully nonlinear parabolic PDEs. *Ann. Appl. Probab.* 21, 4 (2011), 1322–1364.
- [39] FORSYTH, P. A., AND VETZAL, K. R. Implicit solution of uncertain volatility/transaction cost option pricing models with discretely observed barriers. *Appl. Numer. Math.* 36, 4 (2001), 427–445.

- [40] FU, Y., ZHAO, W., AND ZHOU, T. Efficient spectral sparse grid approximations for solving multi-dimensional forward backward SDEs. *Discrete Contin. Dyn. Syst. Ser. B* 22, 9 (2017), 3439–3458.
- [41] GEISS, C., AND LABART, C. Simulation of BSDEs with jumps by Wiener chaos expansion. *Stochastic Process. Appl.* 126, 7 (2016), 2123–2162.
- [42] GEISS, S., AND YLINEN, J. Decoupling on the Wiener space, related Besov spaces, and applications to BSDEs. *arXiv:1409.5322* (2014), 101 pages.
- [43] GOBET, E., AND LABART, C. Solving BSDE with adaptive control variate. *SIAM J. Numer. Anal.* 48, 1 (2010), 257–277.
- [44] GOBET, E., AND LEMOR, J.-P. Numerical simulation of BSDEs using empirical regression methods: theory and practice. *arXiv:0806.4447* (2008), 17 pages.
- [45] GOBET, E., LEMOR, J.-P., AND WARIN, X. A regression-based Monte Carlo method to solve backward stochastic differential equations. *Ann. Appl. Probab.* 15, 3 (2005), 2172–2202.
- [46] GOBET, E., LÓPEZ-SALAS, J. G., TURKEDJIEV, P., AND VÁZQUEZ, C. Stratified regression Monte-Carlo scheme for semilinear PDEs and BSDEs with large scale parallelization on GPUs. *SIAM J. Sci. Comput.* 38, 6 (2016), C652–C677.
- [47] GOBET, E., AND TURKEDJIEV, P. Approximation of backward stochastic differential equations using Malliavin weights and least-squares regression. *Bernoulli* 22, 1 (2016), 530–562.
- [48] GOBET, E., AND TURKEDJIEV, P. Linear regression MDP scheme for discrete backward stochastic differential equations under general conditions. *Math. Comp.* 85, 299 (2016), 1359–1391.
- [49] GUO, W., ZHANG, J., AND ZHUO, J. A monotone scheme for high-dimensional fully nonlinear PDEs. *Ann. Appl. Probab.* 25, 3 (2015), 1540–1580.
- [50] GUYON, J., AND HENRY-LABORDÈRE, P. The uncertain volatility model: a Monte Carlo approach. *The Journal of Computational Finance* 14, 3 (2011), 37–61.
- [51] HAN, J., AND E, W. Deep Learning Approximation for Stochastic Control Problems. *arXiv:1611.07422* (2016), 9 pages.
- [52] HAN, J., JENTZEN, A., AND E, W. Overcoming the curse of dimensionality: Solving high-dimensional partial differential equations using deep learning. *arXiv:1707.02568* (2017), 13 pages.

- [53] HENRY-LABORDÈRE, P. Counterparty risk valuation: a marked branching diffusion approach. *arXiv:1203.2369* (2012), 17 pages.
- [54] HENRY-LABORDÈRE, P., OUDJANE, N., TAN, X., TOUZI, N., AND WARIN, X. Branching diffusion representation of semilinear PDEs and Monte Carlo approximation. *arXiv:1603.01727* (2016), 30 pages.
- [55] HENRY-LABORDÈRE, P., TAN, X., AND TOUZI, N. A numerical algorithm for a class of BSDEs via the branching process. *Stochastic Process. Appl. 124*, 2 (2014), 1112–1140.
- [56] HUIJKENS, T. P., RUIJTER, M. J., AND OOSTERLEE, C. W. Efficient numerical Fourier methods for coupled forward-backward SDEs. *J. Comput. Appl. Math. 296* (2016), 593–612.
- [57] IOFFE, S., AND SZEGEDY, C. *Batch normalization: accelerating deep network training by reducing internal covariate shift*. Proceedings of The 32nd International Conference on Machine Learning (ICML), 2015.
- [58] KARATZAS, I., AND SHREVE, S. E. *Brownian motion and stochastic calculus*, second ed., vol. 113 of *Graduate Texts in Mathematics*. Springer-Verlag, New York, 1991.
- [59] KHOO, Y., LU, J., AND YING, L. Solving parametric PDE problems with artificial neural networks. *arXiv:1707.03351* (2017).
- [60] KINGMA, D., AND BA, J. *Adam: a method for stochastic optimization*. Proceedings of the International Conference on Learning Representations (ICLR), 2015.
- [61] KLOEDEN, P. E., AND PLATEN, E. *Numerical solution of stochastic differential equations*, vol. 23 of *Applications of Mathematics (New York)*. Springer-Verlag, Berlin, 1992.
- [62] KONG, T., ZHAO, W., AND ZHOU, T. Probabilistic high order numerical schemes for fully nonlinear parabolic PDEs. *Commun. Comput. Phys. 18*, 5 (2015), 1482–1503.
- [63] KRIZHEVSKY, A., SUTSKEVER, I., AND HINTON, G. E. Imagenet classification with deep convolutional neural networks. *Advances in Neural Information Processing Systems 25* (2012), 1097–1105.
- [64] LABART, C., AND LELONG, J. A parallel algorithm for solving BSDEs. *Monte Carlo Methods Appl. 19*, 1 (2013), 11–39.

- [65] LAGARIS, I. E., LIKAS, A., AND FOTIADIS, D. I. Artificial neural networks for solving ordinary and partial differential equations. *IEEE Transactions on Neural Networks* 9, 5 (1998), 987–1000.
- [66] LAURENT, J.-P., AMZELEK, P., AND BONNAUD, J. An overview of the valuation of collateralized derivative contracts. *Review of Derivatives Research* 17, 3 (2014), 261–286.
- [67] LECUN, Y., BENGIO, Y., AND HINTON, G. Deep learning. *Nature* 521 (2015), 436–444.
- [68] LECUN, Y., BOTTOU, L., BENGIO, Y., AND HAFFNER, P. Gradient-based learning applied to document recognition. *Proceedings of the IEEE* 86, 11 (1998), 2278–2324.
- [69] LEE, H., AND KANG, I. S. Neural algorithm for solving differential equations. *J. Comput. Phys.* 91, 1 (1990), 110–131.
- [70] LELAND, H. E. Option pricing and replication with transactions costs. *J. Finance* 40, 5 (1985), 1283–1301.
- [71] LEMOR, J.-P., GOBET, E., AND WARIN, X. Rate of convergence of an empirical regression method for solving generalized backward stochastic differential equations. *Bernoulli* 12, 5 (2006), 889–916.
- [72] LIONNET, A., DOS REIS, G., AND SZPRUCH, L. Time discretization of FBSDE with polynomial growth drivers and reaction-diffusion PDEs. *Ann. Appl. Probab.* 25, 5 (2015), 2563–2625.
- [73] MA, J., PROTTER, P., SAN MARTÍN, J., AND TORRES, S. Numerical method for backward stochastic differential equations. *Ann. Appl. Probab.* 12, 1 (2002), 302–316.
- [74] MA, J., PROTTER, P., AND YONG, J. M. Solving forward-backward stochastic differential equations explicitly—a four step scheme. *Probab. Theory Related Fields* 98, 3 (1994), 339–359.
- [75] MA, J., AND YONG, J. *Forward-backward stochastic differential equations and their applications*, vol. 1702 of *Lecture Notes in Mathematics*. Springer-Verlag, Berlin, 1999.
- [76] MARUYAMA, G. Continuous Markov processes and stochastic equations. *Rend. Circ. Mat. Palermo (2)* 4 (1955), 48–90.
- [77] MCKEAN, H. P. Application of Brownian motion to the equation of Kolmogorov-Petrovskii-Piskunov. *Comm. Pure Appl. Math.* 28, 3 (1975), 323–331.

- [78] MEADE, JR., A. J., AND FERNÁNDEZ, A. A. The numerical solution of linear ordinary differential equations by feedforward neural networks. *Math. Comput. Modelling* 19, 12 (1994), 1–25.
- [79] MEHRKANOON, S., AND SUYKENS, J. A. Learning solutions to partial differential equations using LS-SVM. *Neurocomputing* 159 (2015), 105–116.
- [80] MILSTEIN, G. N. Approximate integration of stochastic differential equations. *Teor. Veroyatnost. i Primenen.* 19 (1974), 583–588.
- [81] MILSTEIN, G. N., AND TRETYAKOV, M. V. Numerical algorithms for forward-backward stochastic differential equations. *SIAM J. Sci. Comput.* 28, 2 (2006), 561–582.
- [82] MILSTEIN, G. N., AND TRETYAKOV, M. V. Discretization of forward-backward stochastic differential equations and related quasi-linear parabolic equations. *IMA J. Numer. Anal.* 27, 1 (2007), 24–44.
- [83] MOREAU, L., MUHLE-KARBE, J., AND SONER, H. M. Trading with small price impact. *Math. Finance* 27, 2 (2017), 350–400.
- [84] ØKSENDAL, B. *Stochastic differential equations*. Universitext. Springer-Verlag, Berlin, 1985. An introduction with applications.
- [85] PARDOUX, É., AND PENG, S. Adapted solution of a backward stochastic differential equation. *Systems Control Lett.* 14, 1 (1990), 55–61.
- [86] PARDOUX, E., AND PENG, S. Backward stochastic differential equations and quasi-linear parabolic partial differential equations. In *Stochastic partial differential equations and their applications (Charlotte, NC, 1991)*, vol. 176 of *Lect. Notes Control Inf. Sci.* Springer, Berlin, 1992, pp. 200–217.
- [87] PARDOUX, E., AND TANG, S. Forward-backward stochastic differential equations and quasilinear parabolic PDEs. *Probab. Theory Related Fields* 114, 2 (1999), 123–150.
- [88] PENG, S. Probabilistic interpretation for systems of quasilinear parabolic partial differential equations. *Stochastics Stochastics Rep.* 37, 1-2 (1991), 61–74.
- [89] PENG, S. Nonlinear expectations, nonlinear evaluations and risk measures. In *Stochastic methods in finance*, vol. 1856 of *Lecture Notes in Math.* Springer, Berlin, 2004, pp. 165–253.
- [90] PENG, S. Nonlinear expectations and nonlinear Markov chains. *Chinese Ann. Math. Ser. B* 26, 2 (2005), 159–184.

- [91] PENG, S. G -expectation, G -Brownian motion and related stochastic calculus of Itô type. In *Stochastic analysis and applications*, vol. 2 of *Abel Symp.* Springer, Berlin, 2007, pp. 541–567.
- [92] PENG, S. Nonlinear expectations and stochastic calculus under uncertainty. *arXiv:1002.4546* (2010), 149 pages.
- [93] PHAM, H. Feynman-Kac representation of fully nonlinear PDEs and applications. *Acta Math. Vietnam.* 40, 2 (2015), 255–269.
- [94] POSSAMAÏ, D., METE SONER, H., AND TOUZI, N. Homogenization and asymptotics for small transaction costs: the multidimensional case. *Comm. Partial Differential Equations* 40, 11 (2015), 2005–2046.
- [95] RAMUHALLI, P., UDPA, L., AND UDPA, S. S. Finite-element neural networks for solving differential equations. *IEEE Transactions on Neural Networks* 16, 6 (2005), 1381–1392.
- [96] RASULOV, A., RAIMOVA, G., AND MASCAGNI, M. Monte Carlo solution of Cauchy problem for a nonlinear parabolic equation. *Math. Comput. Simulation* 80, 6 (2010), 1118–1123.
- [97] RUDER, S. An overview of gradient descent optimization algorithms. *arXiv:1609.04747* (2016), 14 pages.
- [98] RUIJTER, M. J., AND OOSTERLEE, C. W. A Fourier cosine method for an efficient computation of solutions to BSDEs. *SIAM J. Sci. Comput.* 37, 2 (2015), A859–A889.
- [99] RUIJTER, M. J., AND OOSTERLEE, C. W. Numerical Fourier method and second-order Taylor scheme for backward SDEs in finance. *Appl. Numer. Math.* 103 (2016), 1–26.
- [100] RUSZCZYNSKI, A., AND YAO, J. A dual method for backward stochastic differential equations with application to risk valuation. *arXiv:1701.06234* (2017), 22.
- [101] SIRIGNANO, J., AND SPILIOPOULOS, K. DGM: a deep learning algorithm for solving partial differential equations. *arXiv:1708.07469* (2017), 7 pages.
- [102] SKOROHOD, A. V. Branching diffusion processes. *Teor. Veroyatnost. i Primenen.* 9 (1964), 492–497.
- [103] TADMOR, E. A review of numerical methods for nonlinear partial differential equations. *Bull. Amer. Math. Soc. (N.S.)* 49, 4 (2012), 507–554.

- [104] THOMÉE, V. *Galerkin finite element methods for parabolic problems*, vol. 25 of *Springer Series in Computational Mathematics*. Springer-Verlag, Berlin, 1997.
- [105] TURKEDJIEV, P. Two algorithms for the discrete time approximation of Markovian backward stochastic differential equations under local conditions. *Electron. J. Probab.* 20 (2015), no. 50, 49.
- [106] VON PETERSDORFF, T., AND SCHWAB, C. Numerical solution of parabolic equations in high dimensions. *M2AN Math. Model. Numer. Anal.* 38, 1 (2004), 93–127.
- [107] WARIN, X. Variations on branching methods for non linear PDEs. *arXiv:1701.07660* (2017), 25 pages.
- [108] WATANABE, S. On the branching process for Brownian particles with an absorbing boundary. *J. Math. Kyoto Univ.* 4 (1965), 385–398.
- [109] WINDCLIFF, H., WANG, J., FORSYTH, P. A., AND VETZAL, K. R. Hedging with a correlated asset: solution of a nonlinear pricing PDE. *J. Comput. Appl. Math.* 200, 1 (2007), 86–115.
- [110] ZHANG, G., GUNZBURGER, M., AND ZHAO, W. A sparse-grid method for multi-dimensional backward stochastic differential equations. *J. Comput. Math.* 31, 3 (2013), 221–248.
- [111] ZHANG, J. A numerical scheme for BSDEs. *Ann. Appl. Probab.* 14, 1 (2004), 459–488.
- [112] ZHAO, W., ZHOU, T., AND KONG, T. High order numerical schemes for second-order FBSDEs with applications to stochastic optimal control. *Commun. Comput. Phys.* 21, 3 (2017), 808–834.